การเตรียมและการพิสูจน์เอกลักษณ์ของอนุภาคไมโครซิลก์เซริซิน

นางสาวศีลิยา หลิ่มโตประเสริฐ

ศูนย์วิทยทรัพยากร
จุฬาลงกรณ์มหาวิทยาลัย

วิทยานิพนธ์นี้เป็นส่วนหนึ่งของการศึกษาตามหลักสูตรปริญญาวิทยาศาสตรมหาบัณฑิต
สาขาวิชาปิโตรเคมีและวิทยาศาสตร์พอลิเมอร์
คณะวิทยาศาสตร์ จุฬาลงกรณ์มหาวิทยาลัย
ปีการศึกษา 2551
ลิขสิทธิ์ของจุฬาลงกรณ์มหาวิทยาลัย

PREPARATION AND CHARACTERIZATION OF SILK SERICIN MICROPARTICLES

Miss Seeliya Limtoprasert

ศูนย์วิทยทรัพยากร

A Thesis Submitted in Partial Fulfillment of the Requirements

for the Degree of Master of Science Program in Petrochemistry and Polymer Science

Faculty of Science

Chulalongkorn University

Academic Year 2008

Copyright of Chulalongkorn University

511666

Thesis Title	PREPARATION AND CHARACTERIZATION OF SILK SERICIN MICROPARTICLES
By	Miss Seeliya Limtoprasert
Field of Study	Petrochemistry and Polymer Science
Thesis Principal Advisor	Associate Professor Sanong Ekgasit, Ph.D.

Accepted by the Faculty of Science, Chulalongkorn University in Partial Fulfillment of the Requirements for the Master's Degree

.....Deputy Dean for Administrative Affairs, Acting Dean, The Faculty of Science

(Associate Professor Vimolvan Pimpan, Ph.D.)

THESIS COMMITTEE

.....Chairman

(Associate Professor Sirirat Kokpol, Ph.D.)

.....Thesis Principal Advisor

(Associate Professor Sanong Ekgasit, Ph.D.)

.....Member

(Assistant Professor Warinthorn Chavasiri, Ph.D.)

.....Member

(Associate Professor Chuchaat Thammacharoen)

.....External Member

(Associate Professor Jatuphorn Wootthikanokkhan, Ph.D.)

ศูนย์วิทยทรัพยากร
จุฬาลงกรณ์มหาวิทยาลัย

ศิลิยา หลิ่มโตประเสริฐ: การเตรียมและการพิสูจน์เอกลักษณ์ของอนุภาคไมโครซิลก์เซริซิน (PREPARATION AND CHARACTERIZATION OF SILK SERICIN MICROPARTICLES) อ. ที่ปรึกษาวิทยานิพนธ์หลัก: รศ. ดร. สนอง เอกสิทธ์, 81 หน้า.

อนุภาคไมโครซิลก์เซริซินเตรียมได้จากการตกตะกอนของสารละลายเซริซินในตัวทำละลายอินทรีย์ (เมทานอล เอทานอล และไอโซโพรพานอล) ที่เตรียมขึ้นด้วยวิธีการใหม่ที่ง่ายในปริมาณมาก โดยสารละลายเซริซินได้จากการลอกกาวเส้นใยไหมด้วยตัวลอกกาว (น้ำกลั่น, โซเดียมไฮโดรเจนคาร์บอเนต และ กรดซิตริก) จากการศึกษาผลของตัวทำละลายอินทรีย์ที่มีต่อลักษณะเฉพาะเชิงโมเลกุลของอนุภาคไมโครเซริซินโดยเทคนิคเอทีอาร์เอฟทีไออาร์ไมโครสเปกโทรสโกปี พบว่าอนุภาคไมโครเซริซินที่ผ่านการตกตะกอนด้วยตัวทำละลายอินทรีย์แสดงการเปลี่ยนแปลงทางโครงสร้างจาก random coil ไปเป็น β-sheet เกิดขึ้น ซึ่งแสดงถึงการเชื่อมโยงกันของพันธะในสายโซ่โมเลกุล และผลของโครงสร้างทุติยภูมิของอนุภาคไมโครซิลก์เซริซินที่เตรียมได้จากการตกตะกอนในเมทานอลมีความเป็น β-sheet มากกว่าโครงสร้างทุติยภูมิของอนุภาคไมโครซิลก์เซริซินที่ได้จากการตกตะกอนในไอโซโพรพานอล แสดงให้เห็นว่าสามารถควบคุมโครงสร้างทุติยภูมิของอนุภาคไมโครซิลก์เซริซินได้ด้วยตัวทำละลายอินทรีย์ตั้งแต่ขั้นตอนการเตรียม ผลของการวิเคราะห์ขนาดและรูปร่างของอนุภาค ไมโครซิลก์เซริซินโดยใช้กล้องจุลทรรศน์อิเล็กตรอนแบบส่องกราด พบว่าขนาดอนุภาคของตะกอนเซริซินอยู่ในรูปอนุภาคไมโครซึ่งมีขนาดอนุภาคเฉลี่ยประมาณ 5 ไมโครเมตรแต่ยังไม่แยกตัวกันอย่างสมบูรณ์เนื่องจากลักษณะเฉพาะของเซริซิน นอกจากนี้เราสามารถนำอนุภาคไมโครซิลก์เซริซินที่เตรียมได้มาประยุกต์ใช้ในการเป็นตัวรองรับอนุภาคนาโนเงิน ผลการศึกษาพบว่าอนุภาคนาโนเงินสามารถกระจายตัวและเกาะอยู่บนอนุภาคไมโครซิลก์เซริซินได้ดีมาก

ศูนย์วิทยทรัพยากร
จุฬาลงกรณ์มหาวิทยาลัย

สาขาวิชา ปิโตรเคมีและวิทยาศาสตร์พอลิเมอร์ ลายมือชื่อนิสิต ศิลิยา หลิ่มโตประเสริฐ
ปีการศึกษา 2551 ลายมือชื่ออาจารย์ที่ปรึกษาวิทยานิพนธ์หลัก

4972510523 : MAJOR PETROCHEMISTRY AND POLYMER SCIENCE
KEY WORDS : ATR FT-IR MICROSPECTROSCOPY, SILK SERICIN MICROPARTICLES

SEELIYA LIMTOPRASERT: PREPARATION AND CHARACTERIZATION OF SILK SERICIN MICROPARTICLES. THESIS PRINCIPAL ADVISOR: ASSOC. PROF. SANONG EKGASIT, PH.D., 81 pp.

Silk sericin microparticles are obtained from precipitation of sericin solution in organic solvent (methanol, ethanol and *iso*-propanol) which develops a novel technique for preparation silk sericin microparticles in mass scale. The solution was prepared from boiling solution of silk fiber with degumming agent (distilled water, sodium hydrogen carbonate, and citric acid). Effects of organic solvent on the molecular characteristics of silk sericin microparticles were investigated by Attenuated Total Reflection Fourier Transform Infrared (ATR FT-IR) spectroscopy. The results of ATR FT-IR spectra elucidated that the conformation of the silk sericin microparticles were changed from random coil to β-sheet after treatment. The appearance of β-sheet conformation may be associated with the packing of molecular chains. The secondary structure of silk sericin microparticles treated in methanol had more β-sheet structure than that treated in *iso*-propanol. The results indicated that the secondary structure of silk sericin microparticles could be controlled by organic solvent from the preparation. The morphology of silk sericin microparticles was observed by scanning electron microscope. The average particle size of silk sericin microparticles were about 5 μm but it does not completely isolate arising from its native structure. Silk sericin microparticles can apply for silver nanoparticles deposition. Silver nanoparticles are very well dispersed and deposited on silk sericin microparticles.

ศูนย์วิทยทรัพยากร
จุฬาลงกรณ์มหาวิทยาลัย

Field of study Petrochemistry and Polymer Science Student's signature ลีลิยา ลิมโทปราเสริฐ
Academic year 2008 Principal Advisor's signature

ACKNOWLEDGEMENTS

I would like to express my sincere gratitude to Associate Professor Dr. Sirirat Kokpol, Assistant Professor Dr. Warinthorn Chavasiri, and Associate Professor Dr. Jatuphorn Wootthikanokkhan for suggestions and contributions as thesis committee.

Gratefully thanks to Associate Professor Dr. Sanong Ekgasit, my thesis advisor and Associate Professor Chuchaat Thammacharoen, for the invaluable guidance, comments, and suggestions, encouragement, and understanding and also patiently practices my technical skill during the whole research.

The authors would like to acknowledge Mr. Wonchalerm Rungswang and Associate Professor Dr. Suwabun Chirachanchai for the morphological characterization using transmission electron microscope technique. Mr. Prateep Meesilpa, Director of The Queen Sirikit Institute of Sericulture, Office of the Permanent Secretary for Agriculture and Cooperatives, Ministry of Agriculture and Cooperatives for silk fiber supply and National Center of Excellence for Petroleum, Petrochemicals, and Advanced Materials, NCE-PPAM and the Commission of higher Education for partial financial supports.

Above all, I am profoundly grateful to my wonderful parents and the endearing family for their patient love, perpetual encouragement, and overwhelming support.

ศูนย์วิทยทรัพยากร
จุฬาลงกรณ์มหาวิทยาลัย

CONTENTS

Page

ABSTRACT (IN THAI)..... iv
ABSTRACT (IN ENGLISH)..... v
ACKNOWLEDGEMENTS..... vi
LIST OF FIGURES..... xi
LIST OF TABLES..... xv
LIST OF ABBREVIATIONS..... xvi
LIST OF SYMBOLS..... xvii

CHAPTER I INTRODUCTION..... 1

1.1 Native silk sericins..... 1
1.2 Silk sericin microparticles..... 3
1.3 ATR FT-IR microspectroscopy of silk sericin..... 4
1.4 The objectives of this research 4
1.5 The scopes of this research 5
1.6 Expected benefits..... 5

CHAPTER II THEORETICAL BACKGROUND..... 6

2.1 Silkworm 6
2.2 Silk gland..... 7
2.3 Silk fiber..... 8
2.4 Structure of protein..... 10
2.4.1 Primary structure..... 11
2.4.2 Secondary structure..... 11
2.4.2.1 α-helix..... 11
2.4.2.2 The β-strand..... 12
2.4.2.3 β-turn..... 13
2.4.2.4 Random coil..... 14
2.4.3 Tertiary structure..... 15

ศูนย์วิทยทรัพยากร
จุฬาลงกรณ์มหาวิทยาลัย

Page

2.4.4 Quaternary structure..... 15
2.5 Analysis of protein spectra to obtain secondary structural information..... 16
2.6 Infrared spectroscopy..... 16
2.6.1 Principles of light reflection and refraction..... 18
2.7 Attenuated Total Reflection Fourier Transform Infrared (ATR FT-IR) Spectroscopy..... 18
2.7.1 Internal reflection Element (IRE)..... 20
2.7.2 Limitation of ATR FT-IR spectroscopy..... 21
2.7.3 Homemade Slide-on Ge IRE Accessory..... 21

CHAPTER III EXPERIMENTAL SECTION..... 23

3.1 Materials..... 23
3.1.1 Silk fiber..... 23
3.1.2 Chemicals..... 23
3.1.3 Organic solvents..... 23
3.1.4 Silver nanoparticles..... 24
3.2 Experimental section..... 24
3.2.1 Preparation of silk sericin microparticles..... 24
3.3 Characterization of silk sericin microparticles..... 25
3.3.1 Attenuated Total Reflection Fourier Transform Infrared (ATR FT-IR) microspectroscopy..... 25
3.3.2 Scanning electron microscope (SEM)..... 29
3.4 The deposition of silver nanoparticles on silk sericin microparticles..... 30
3.4.1 UV-visible spectroscopy..... 30
3.4.2 Transmission electron microscope (TEM)..... 32

CHAPTER IV RESULTS AND DISCUSSION..... 33

4.1 Silk sericin microparticles..... 33
4.2 The Morphology of native silk sericin and silk sericin microparticles..... 34

Page

4.3 ATR FT-IR of native silk sericin..... 36
4.4 Structural information of native silk sericin..... 36
4.5 ATR FT-IR spectra of native silk sericin and silk fibroin fiber..... 38
4.6 Secondary structure of native silk sericin and silk fibroin fiber analyzed by ATR FT-IR spectroscopy..... 40
4.7 Characterization of silk sericin solutions and silk sericin microparticles 44
4.7.1 ATR FT-IR spectra of slurry, sericin solution, and yellow fibril sericin..... 44
4.7.2 ATR FT-IR spectra of silk sericin microparticles..... 46
4.7.3 Secondary structure of silk sericin microparticles analyzed by ATR FT-IR microspectroscopy 49
4.8 ATR FT-IR spectra of native silk sericin and silk sericin microparticles obtained from precipitating in methanol..... 58
4.9 The deposition of silver nanoparticles on silk sericin microparticles..... 59
4.9.1 TEM images of silver nanoparticles deposited on silk sericin microparticles..... 60
4.9.2 The ATR FT-IR spectra of silk sericin microparticles before and after added silver nanoparticles 61
4.9.3 UV-Vis spectra of silver nanoparticles before and after deposited on silk sericin microparticles and the release of silver nanoparticles deposited on silk sericin microparticles..... 62
4.10 UV-Vis spectra of silver nanoparticles at different concentrations..... 64
4.11 Amount of the deposition of silver nanoparticles on silk sericin microparticles and the release of silver nanoparticles deposited on silk sericin microparticles..... 66
CHAPTER V CONCLUSIONS..... 69
REFERENCES..... 71

Page

APPENDICES..... 76

CURRICULUM VITAE..... 81

ศูนย์วิทยทรัพยากร
จุฬาลงกรณ์มหาวิทยาลัย

LIST OF FIGURES

Figure		Page
1.1	The structures of silk fiber	2
2.1	Silkworm life cycle.....	7
2.2	Silk glands of mature, larva, *Bombyx mori*.....	8
2.3	An example of the primary structure of protein.....	11
2.4	Arrangement of hydrogen bonds backbone of α-helix.....	12
2.5	Two adjacent β-strands are hydrogen bonded form a small element of β-sheet forms: (a) Parallel β-sheet and (b) Anti-Parallel β-sheet.....	13
2.6	Arrangement of β-turn structure.....	14
2.7	Arrangement of atom in β-turns: (a) Type I and (b) Type II.....	14
2.8	Arrangement of random coil sructure.....	15
2.9	Four levels of protein structure; primary, secondary, tertiary, and quaternary structures.....	16
2.10	Interaction of light with matter	17
2.11	Reflection and refraction of a plane wave at a dielectric interface based on Snell's law.	18
2.12	Light travels from an optically denser medium and impinges at the surface of the optically rarer medium ($n_1 > n_2$) with angle of incidence equals the critical angle.....	19
2.13	IRE configurations commonly used in ATR experimental setups: (a) Single reflection variable-angle hemispherical crystal and (b) Multiple reflection single-pass crystal.....	21
2.14	The infrared radiation tracing within the Ge μIRE.....	22
3.1	Schematic illustrations of preparation silk sericin microparticles obtained from boiling solution of silk fiber by (A) distilled water, (B) citric acid, and (C) $NaHCO_3$.....	25
3.2	Schematic diagram of ATR measurement configuration	28

Figure Page

3.3 ATR FT-IR microspectroscope: (A) Continuμm® infrared microscope coupled with the Nicolet 6700 FT-IR spectrometer, (B) the slide-on Ge μIRE is fixed on the position of slide-on housing on the infrared objective, and (C) Homemade slide-on germanium (Ge) μIRE..... 29
3.4 Scanning electron microscope (SEM)..... 29
3.5 UV-Visible spectrometer 31
3.6 Hitashi H-7650 transmission electron microscope..... 32
4.1 Silk sericin microparticles obtained from solution of silk fiber degumming with (A) distilled water, (B) citric acid, and (C) $NaHCO_3$ after treating with organic solvents: (a) methanol, (b) ethanol, and (c) *iso*-propanol..... 34
4.2 SEM images of (A) native silk sericin at three different positions, silk sericin microparticles obtained from precipitation of sericin solution boiled with (B) distilled water, (C) citric acid, and (D) $NaHCO_3$ in organic solvents: (a) methanol, (b) ethanol, and (c) *iso*-propanol..... 35
4.3 ATR FT-IR spectrum of native silk sericin..... 37
4.4 ATR FT-IR spectra of native silk sericin from a single silk fiber collected at three different positions. The inset is the normalized spectra..... 37
4.5 ATR FT-IR spectra of (a) native silk sericin and (b) silk fibroin fiber..... 39
4.6 Curve fitting of (A) native silk sericin, and (B) silk fibroin fiber spectra in the Amide I region: (a) second derivative spectrum, (b) deconvolved (solid line) spectrum, and (c) original (dotted line) spectrum..... 42
4.7 ATR FT-IR spectra of silk sericin degumming with (A) distilled water, and (B) citric acid: (a) slurry, (b) sericin solution, and (c) yellow fibril sericin; ATR FT-IR spectra of sericin degumming with (C) $NaHCO_3$: (a) sericin solution and (b) sericin solution after adding NaCl..... 45
4.8 ATR FT-IR spectra of sericin microparticles obtained from boiling solution of silk fiber with (A) distilled water, (B) citric acid, and (C) $NaHCO_3$ treated with different organic solvents: (a) methanol, (b) ethanol, and (c) *iso*-propanol. The inset is the normalized spectra in Amide I region..... 47

Figure Page

4.9 Curve fitting of silk sericin microparticles spectra in the Amide I region obtained from boiling solution of silk fiber with distilled water after treated with (A) methanol, (B) ethanol, and (C) *iso*-propanol: (a) second derivative spectrum, (b) deconvolved (solid line) spectrum, and (c) original (dotted line) spectrum..... 50

4.10 Curve fitting of silk sericin microparticles spectra in the Amide I region obtained from boiling solution of silk fiber with citric acid after treated with (A) methanol, (B) ethanol, and (C) *iso*-propanol: (a) second derivative spectrum, (b) deconvolved (solid line) spectrum, and (c) original (dotted line) spectrum..... 52

4.11 Curve fitting of silk sericin microparticles spectra in the Amide I region obtained from boiling solution of silk fiber with $NaHCO_3$ after treated with (A) methanol, (B) ethanol, and (C) *iso*-propanol: (a) second derivative spectrum, (b) deconvolved (solid line) spectrum, and (c) original (dotted line) spectrum..... 55

4.12 ATR FT-IR spectra of (a) native silk sericin; silk sericin microparticles obtained from precipitation of sericin solution in methanol with different degumming agent: (b) distilled water, (c) citric acid, and (d) $NaHCO_3$. The inset is the normalized spectra in Amide I region..... 59

4.13 The deposited of silver nanoparticles on silk sericin microparticles with concentrations: (a) 50, (b) 100, and (c) 200 ppm 60

4.14 Transmission electron microscope (TEM) images of (A) silk sericin microparticles and the silver nanoparticles deposited on silk sericin microparticles with concentrations (B) 50, (C) 100, and (D) 200 ppm..... 61

4.15 ATR FT-IR spectra of (a) silk sericin microparticles and silver nanoparticles deposited on silk sericin microparticles with concentrations: (b) 50, (c) 100, and (d) 200 ppm..... 62

4.16 UV-Vis absorption spectra of (A) 50, (B) 100, and (C) 200 ppm silver nanoparticles: (a) reference, (b) silver nanoparticles residue in distilled water, and (c) the release of silver nanoparticles deposited on silk sericin microparticles..... 63

Figure Page

4.17 UV-Vis absorption spectra of silver nanoparticles at different concentrations of (a) 0.05, (b) 0.25, (c) 0.5, (d) 1.5, (e) 2.5, (f) 3.5, (g) 5, (h) 6.5, (i) 8, and (j) 10 ppm..... 64
4.18 Calibration curve of silver nanoparticles at different concentrations..... 65

ศูนย์วิทยทรัพยากร
จุฬาลงกรณ์มหาวิทยาลัย

LIST OF TABLES

Table		Page
2.1	Composition of silk in *Bombyx mori*	8
2.2	Amino acid composition of silk sericin (mole %)	10
2.3	Information of materials used for internal reflection elements	21
4.1	Particles size of silk sericin microparticles	36
4.2	Peak assignments of native silk sericin and silk fibroin fiber in comparison with the literatures	40
4.3	Carbonyl absorption associated with the secondary structure of native silk sericin and silk fibroin	43
4.4	Peak assignments of silk sericin microparticles	48
4.5	Carbonyl absorption associated with the secondary structure of silk sericin microparticles obtained from boiling solution of silk fiber with distilled water after treatment with different organic solvents.	51
4.6	Carbonyl absorption associated with the secondary structure of silk sericin microparticles obtained from boiling solution of silk fiber with citric acid after treatment with different organic solvents	53
4.7	Carbonyl absorption associated with the secondary structure of silk sericin microparticles obtained from boiling solution of silk fiber with $NaHCO_3$ after treatment with different organic solvents	56
4.8	The average yield of silk sericin microparticles treated with organic solvents	57
4.9	The absorbance of UV-Vis spectra of silver nanoparticles at different concentrations	65
4.10	Deposition of silver nanoparticles on silk sericin microparticles	67
4.11	The release of silver nanoparticles after deposition on silk sericin microparticles	67
4.12	The summary of deposition and release of silver nanoparticles on silk sericin microparticles	68

ศูนย์วิทยทรัพยากร
จุฬาลงกรณ์มหาวิทยาลัย

LIST OF ABBREVIATIONS

Ala	: Alanine
ATR	: Attenuated total reflection
C	: Carbon
CH_2	: Ethylene
FSD	: Fourier self-deconvolution
FT-IR	: Fourier transform infrared
Ge	: Germanium
Gly	: Glycine
H	: hydrogen
IR	: Infrared
IRE	: Internal reflection element
kV	: Kilovolt (10^3 V)
MCT	: Mercury-cadmium-telluride
µg	: Microgram (10^{-6} g)
µm	: Micrometer (10^{-6} m)
MWCO	: Molecular weight cut off
mL	: Milliliter (10^{-3} L)
nm	: Nanometer (10^{-9} m)
N	: nitrogen
O	: oxygen
ppm	: Part per million
SEM	: Scanning electron microscopy
Ser	: Serine
NaCl	: Sodium chloride
$NaHCO_3$	: Sodium hydrogen carbonate
TEM	: Transmission electron microscopy
vdW	: van der Waals
W/W	: Weight per weight
W/V	: Weight per volume
ZnSe	: Zinc selenide

ศูนย์วิทยทรัพยากร
จุฬาลงกรณ์มหาวิทยาลัย

LIST OF SYMBOLS

A	: Absorbance
ε	: Absorption coefficient
α	: Alpha
α_1	: Angle of incidence
α_2	: Angle of reflection
θ	: Angle of incidence
β	: Beta
℃	: Celsius
θ_c	: Critical angle
c	: Concentration
l	: Film thickness
I_0	: Intensity of incident beam
I_R	: Intensity of reflected beam
I_S	: Intensity of scattered beam
I_T	: Intensity of transmitted beam
I_A	: Intensity of absorbed beam
I	: Light intensity
μ	: Micron (10^{-6} m)
d_p	: Penetration depth
n_1	: Refractive index of the dense medium (IRE)
n_2	: Refractive index of the sample
ν	: Wavenumber
λ	: Wavelength

ศูนย์วิทยทรัพยากร
จุฬาลงกรณ์มหาวิทยาลัย

CHAPTER I

INTRODUCTION

Silk is a natural protein fiber that mainly consists of sericin and fibroin proteins. It is produced from cocoon of silkworm *Bombyx mori*. Silk cocoon contains 70-80% of silk fibroin protein and 20-30% of sericin protein. In fabric industries, silk fiber is one of popular raw material. Sericin or "silk gum" would be eliminated or degummed in fabric process and it becomes waste. There are many researches that try to recover and utilize sericin from degumming process [1-3]. The recovery of sericin has found effective applications for many purposes such as textiles, medical, and cosmetic applications, etc [4-7].

1.1 Native silk sericins

In native silk fiber, sericin is formed to be layers covering fibroin fiber. The sericin layers are formed from the outside to inside. Sericin is a complex protein composed of three distinct components, so-called "Sericin I, II, III", which have different solubilities in hot water. The outer layer is the Sericin I, and the inner layers are Sericin II and III. Moreover, it has been found that Sericin I on the cocoon filament is amorphous where as Sericin II and III are crystalline [8]. The structures of silk fiber were shown in Figure 1.1.

The molecular weight of sericin is in the ranges of 10 to over 300 kDa [1, 4]. Sericin is a macromolecular protein that consists of 18 amino acids. Most of these amino acids have strong polar side groups such as hydroxyl, carboxyl and amino groups. Especially, serine and aspartic acid, which are hydrophilic amino acid, approximately constitute 33.4% and 16.7% of serine, respectively. The sericin peptides are widely useful in medical industry and beauty treatment [4-7, 9-10]. For examples low molecular weight sericin peptides are utilized in controlled drug delivery, hydrogels, and cosmetics for skincare and haircare, and health products [4]. On the other hand, the higher molecular weight sericin peptides can be applied to medical, degradable biomaterials, polymers compound, biomembranes, and functional fibers and fabrics [4-7, 9-10]. Sericin has also shown several extraordinary properties

e.g., it can resist oxidation, UV radiation [2, 10] and exhibits antibacterial activities [11]. Moreover, it can adsorb and release moisture easily. Sericin is a valuable ingredient for cosmetics because it can inhibit tyrosinase activity which is responsible for biosynthesis of skin melanin [12].

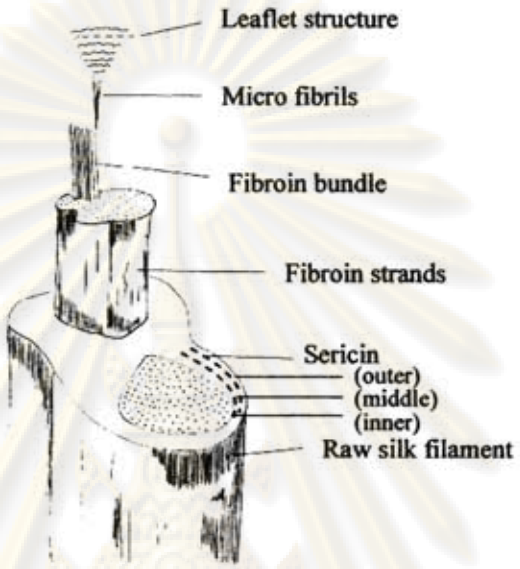

Figure 1.1 The structures of silk fiber [13].

The sericin envelops fibroin fibers in the form of successive sticky layers. The most of the silk sericin must be removed from silk fibroin fiber by ***"Silk degumming or Boiling off"*** processes. It is mostly discarded in silk processing wastewater [14]. When the sericin protein flows into river, the environment is destroyed [15]. Recently, many researchers have studied the structure and morphology of sericin in order to refine the sericin from waste water [3]. Silk waste has the physical and chemical properties similar to silk cocoon, i.e., it contains fibroin and sericin proteins. Teramoto H. et al. have studied the structure of native silk sericin and reported disordered structures in protein [16]. This indicated that forming of orient sericin molecules was difficult to occur. Since silk sericin cannot be used to make fabric as the same for silk fibroin, the technique for preparation of silk sericin in microparticles form is developed. The microparticles were simply prepared by precipitation of sericin solution in organic solvents at room temperature. Recovery of this useful protein from silk waste into particle-forms provides a wide range of application such

as cosmetics, hair care, drug delivery, and oxidation resistance agents of oil and fat [13, 17].

1.2 Silk sericin microparticles

The sericin solution removed from silk degumming process is waste of silk industry. It could be formed into micro-structures. The size of silk sericin microparticles are in the range of 1-100 μm. Lee et al. prepared silk sericin powder by freezing and lyophilizing of sericin solution. The authors reported the morphology changes of silk sericin from sheet-like structure to spherical fine particles after added methanol [18]. Structural change of silk sericin from random coil to β-sheet was reported by Cho et al. They obtained the silk sericin nanoparticles by reacting sericin solution with poly (ethylene glycol). The shapes of nanoparticles were almost spherical with nano-scaled size [17]. Later on, Teramoto et al. used ethanol to prepare sericin film, and observed the aggregated strands with strong intermolecular hydrogen bonds in the structures of protein [19]. Wu et al. also pointed out the structural change of silk sericin, which was changed from random coil to β-turn structure after treated with ethanol [2]. Kurioka et al. prepared silk sericin powder by lyophilizing of sericin solution with degumming agent. The author found that the size of sericin powder (1-10 μm) obtained after degummed with citric acid was smaller than those obtained by degumming with distilled water and sodium bi-carbonate [20]. Although several methods for preparation sericin particles have been proposed but none of them seems to be satisfied, because the procedures of preparation were complicated and instruments were expensive. Moreover, the obtained sericin particles were easy to be damaged.

In this study, silk sericin microparticles with precipitation silk sericin solution in organic solvents (methanol, ethanol, *iso*-propanol) were applied with this method, the secondary structure of silk sericin microparticles could be controlled by treated with the organic solvents.

ศูนย์วิทยทรัพยากร
จุฬาลงกรณ์มหาวิทยาลัย

1.3 ATR FT-IR microspectroscopy of silk sericin

In this study, infrared spectroscopy is an invaluable technique to obtain the structural in formations of protein in any environments. The native silk sericin, silk fibroin fiber, silk sericin solution, and silk sericin microparticles were analyzed by means of Attenuated Total Reflection Fourier Transform Infrared (ATR FT-IR) spectroscopy. ATR FT-IR spectroscopy is one of FT-IR sampling techniques that provide molecular information of sample surface. However, due to the limitation of the commercial ATR accessory, a homemade diamond μATR accessory and a homemade Ge μATR accessory were developed by Sensor Research Unit, Department of Chemistry, Faculty of Science, Chulalongkorn University. The advantages of this technique are requirement minute amount of sample and non-destructive technique. In such manner, we can obtain the information about structural changes of silk sericin microparticles during preparation.

Molecular orientation of native silk sericin and silk fibroin fiber were compared. It was found that the native silk sericin was almost random oriented in its structure, which was different from silk fibroin. The observed ATR FT-IR spectra of the silk sericin microparticles after treated with methanol, ethanol, and *iso*-propanol indicated the increment of β-sheet conformation, which might be due to the packing of molecular chain. This study elucidated the molecular orientation behavior of sericin microparticles treated with organic solvents. In the future, we are also interested in producing sericin microparticles, which will be more suitable for the advance application than the native sericin.

1.4 The objectives of this research

1. To investigate the appropriate process for preparation of silk sericin microparticles
2. To develop a novel technique for preparation silk sericin microparticles in mass scale.
3. To determine the characteristics of silk sericin solution obtained from different silk degumming.

ศูนย์วิทยทรัพยากร
จุฬาลงกรณ์มหาวิทยาลัย

4. To determine the characteristics of native silk sericin and silk sericin microparticles.

1.5 The scopes of this research

1. Developing technique for preparation of silk sericin microparticles.
2. Studying the effect of organic solvents treatment on molecular conformation of silk sericin microparticles.
3. Comparison the molecular characteristic and secondary structure of native silk sericin and silk sericin microparticles.
4. Depositing of silver nanoparticles on silk sericin microparticles

1.6 Expected benefits

1. Obtaining a novel and simple method for silk recovery.
2. Preparations silk sericin microparticles.

ศูนย์วิทยทรัพยากร
จุฬาลงกรณ์มหาวิทยาลัย

CHAPTER II

THEORETICAL BACKGROUND

2.1 Silkworm

Like most insects, silkworm undergoes four stages: egg, larva, pupa and adult. Larva is the silkworm caterpillar. The pupa is the state that silkworm changed after spinning its cocoon before emerging as a moth. The adult stage is the silkworm moth. To complete the silkworm life cycle, it must shed its skin four times while growing. These stages-within-a-stages are called instars.

Four states of metamorphosis of silkworm:

1. ***Stages I*** the female moth lays many tiny eggs. A tiny black caterpillar hatches out of its egg then develops into silkworm caterpillars.

2. ***Stage II*** the caterpillar eats mulberry leaves and grows bigger and bigger. It goes through 4 molts. Larvae spin the filament fiber to make their cocoons for protection and metamorphosis into the pupae.

3. ***Stage III*** the caterpillar spin a cocoon of silk threads around itself. Papa emerges from the cocoons as moths.

4. ***Stage IV*** the pupa changes to a moth. The moth comes out of the cocoon. The male and female moths breed and the female moth lays eggs. After that, the eggs will continue the next life cycle. The silkworm life cycle is shown in Figure 2.1. The silk sericin is received from this cocoon.

ศูนย์วิทยทรัพยากร
จุฬาลงกรณ์มหาวิทยาลัย

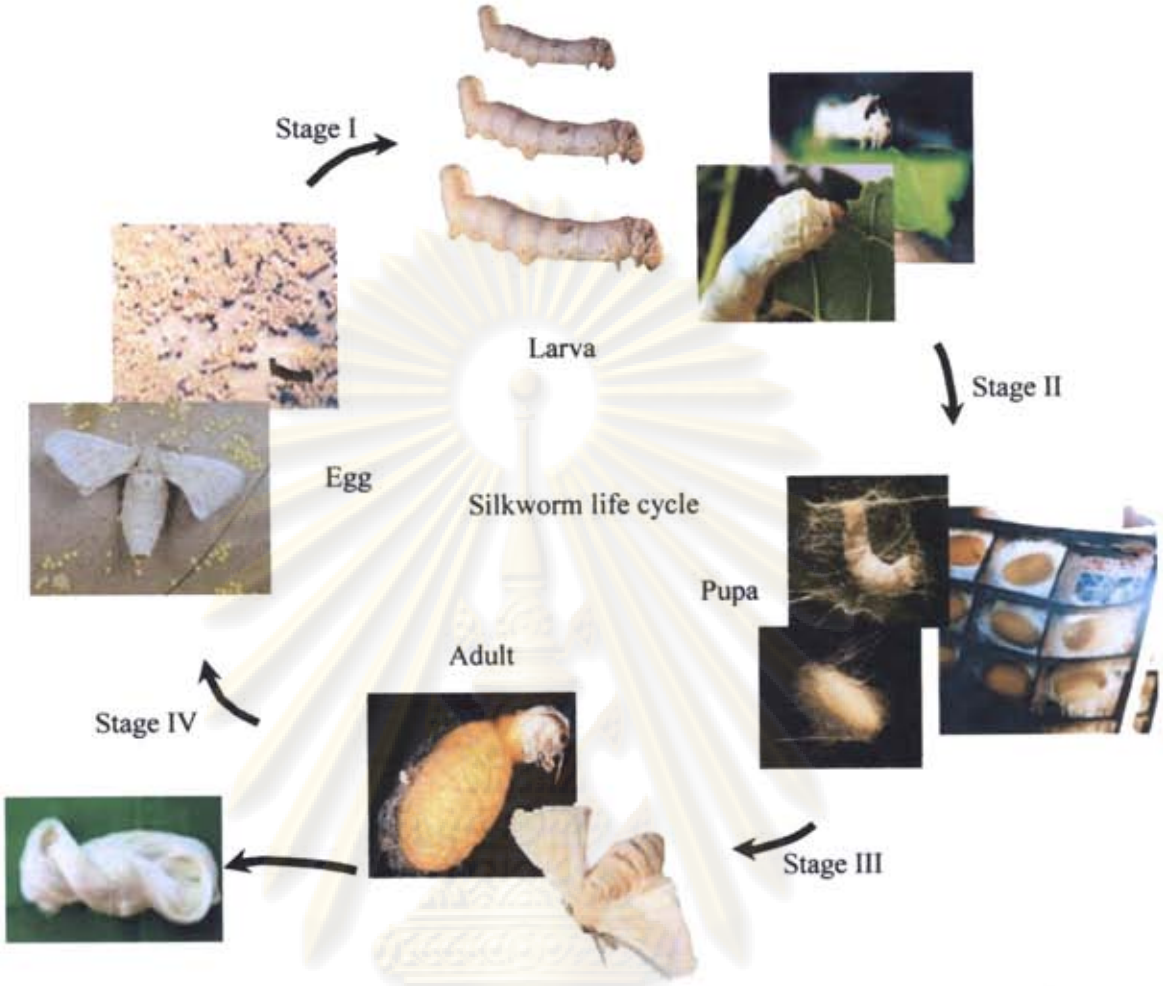

Figure 2.1 Silkworm life cycle [21].

2.2 Silk gland

The natural silk synthesized by the silkworm and spun in the form of a silk cocoon is originally synthesized in the silk gland [22]. The silk producing glands of *Bombyx mori* are long and divided into three distinct regions. The silk glands of mature, larva, ***Bombyx mori*** is shown in Figure 2.2 [23]. The fibroin protein is synthesized in the posterior silk gland, and sericin is produced by the middle silk gland. The two components together in anterior region of the gland are spun into the air and producing a continuous filament.

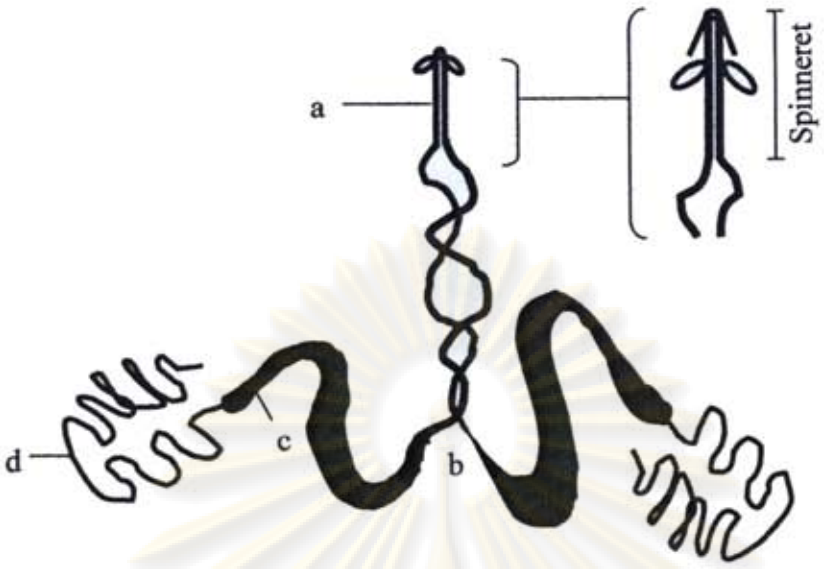

Anterior division (a-b) about 4 cm long and 0.05-0.3 mm wide.
Middle division (b-c) about 8 cm long and 1.2-2.5 mm wide.
Posterior division (c-d) about 20 cm long and 0.4-0.8 cm wide.

Figure 2.2 Silk glands of mature, larva, *Bombyx mori* [23].

2.3 Silk fiber

As a consequence of this spinning process, the silk fiber is almost a pure protein fiber composed of two types of proteins, sericin and fibroin. The components of sericin include protein, lipid, carbohydrate, organic, water, and wax. The percent compositions of silk in *Bombyx mori* are shown in Table 2.1.

Table 2.1 Composition of silk in *Bombyx mori* [24].

Component	%
Fibroin	70-80
Sericin	20-30
Wax matter	0.4-0.8
Carbohydrates	1.2-1.6
Inorganic matter	0.7
Pigment	0.2
Total	100

ศูนย์วิทยทรัพยากร
จุฬาลงกรณ์มหาวิทยาลัย

Silk protein produced from cocoon of silkworm *Bombyx mori* that mainly composed of sericin and fibroin proteins. In case of *Bombyx mori*, silk sericin content is about 20-30 percent. Most of sericin must be removed from silk fibroin and silk threads by ***"Silk degumming or Boiling-off"*** processes [14]. After degumming, the fibroin is obtained. The mechanism of sericin removal in chemical degumming is a combination of various effects such as dispersion/solubilization and hydrolysis of the different sericin polypeptides [25]. There are many suitable procedures eliminating sericin without damaging fibroin. In general, process is performed by using Marseilles soap or synthetic detergent solutions at a temperature of 95-98 ^{O}C. Moreover, some acids such as sulphuric, hydrochloric, tartaric and citric acids [20] can be used as degumming agents. Strong hot caustic alkaline will readily dissolve the fibre. Zhang et al. have reported that the alkaline degumming process, sericin is degrade or hydrolysate into sericin peptide with molecular weight less than 20 kDa [26]. The alkalines used for degumming are sodium carbonate, caustic soda, and sodium bicarbonate. An alkaline reaction at pH>8.5 are most favorable for rapid elimination of sericin [27]. Nowadays, enzymes at 50-60 ^{O}C or simply water at about 130 ^{O}C under high pressure are also used. During the degumming process, fats, oils, and the other substances are removed.

The composition of sericin is distinctly different from fibroin. Sericin is made of 18 amino acids, most of which have strongly polar side groups such as hydroxyl, carboxyl, and amino groups. Sericin is rich in serine, aspartic acid, and glycine, constituting approximately 31.9%, 13.8%, and 12.7% of cocoon sericin, respectively. The different proportions of amino acids in cocoon and gland sericin are shown in Table 2.2.

ศูนย์วิทยทรัพยากร
จุฬาลงกรณ์มหาวิทยาลัย

Table 2.2 Amino acid composition of silk sericin (mole %) [23].

Amino acids	*Bombyx mori*	
	Cocoon	Gland
Glycine	12.70	14.7
Alanine	5.51	4.3
Valine	2.68	3.6
Leucine	0.72	1.4
Isoleucine	0.55	0.7
Serine	31.97	37.3
Threonine	8.25	8.7
Aspatic acid	13.84	14.8
Glutamic acid	5.80	3.4
Lysine	3.26	2.4
Arginine	2.86	3.60
Histidine	1.30	1.2
Tyrosine	3.40	2.6
Phenylalanie	0.43	0.3
Proline	0.57	0.7
Tryptophan	-	-
Methionine	0.05	-
$(Cysteine)_2$	0.14	0.15

2.4 Structure of protein

Protein is constituted from amino acids, which are linked together by peptide bonds. The basic structure of an amino acid molecule consists of a centre carbon atom bonded to an amino group ($-NH_2$), a carboxyl group (-COOH), a hydrogen atom, and a side chain (R). Identify of particular amino acids depends on the nature of R group. Amino acid chains of proteins fold into unique three dimensional structures, and four levels of protein structures are classified; primary, secondary, tertiary and quaternary structures (Figure 2.9).

2.4.1 Primary structure

The primary structure is the linear sequence of amino acid residues along the polypeptide chain that is covalently linked from individual amino acids via peptide bonds (Figure 2.3).

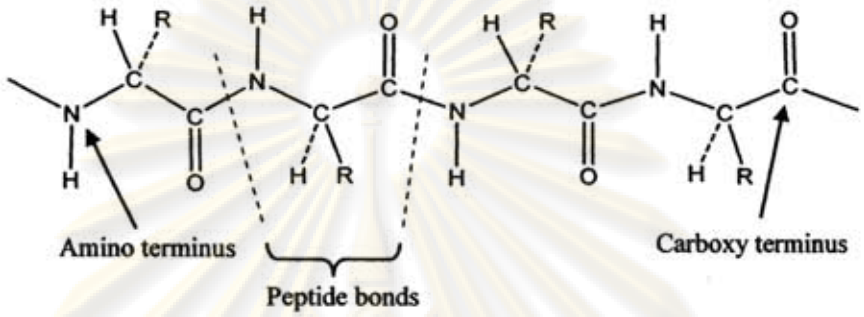

Figure 2.3 An example of the primary structure of protein.

2.4.2 Secondary structure

The secondary structure is a local conformation of the polypeptide chain or the spatial relationship of amino acid residues that are close together in the primary sequence. Four common secondary structure elements in proteins are the α-helix, the β-strand, β-turns, and random coil.

2.4.2.1 α-helix

The α-helix is the most identifiable element of secondary structure. It is stabilized by hydrogen bonds between the carbonyl (C=O) group of one residue and the amide group (NH) of the fourth residues ahead in the polypeptide chain, as shown in Figure 2.4. In principle, the amino end of the α-helix is positively charge whilst the carboxyl end is negatively charge. In the α-helix, the first four NH groups and the last four groups is normally lacked of hydrogen bonds backbone. For this reason, very short helices often have distorted conformations and forms alternative hydrogen bond partners.

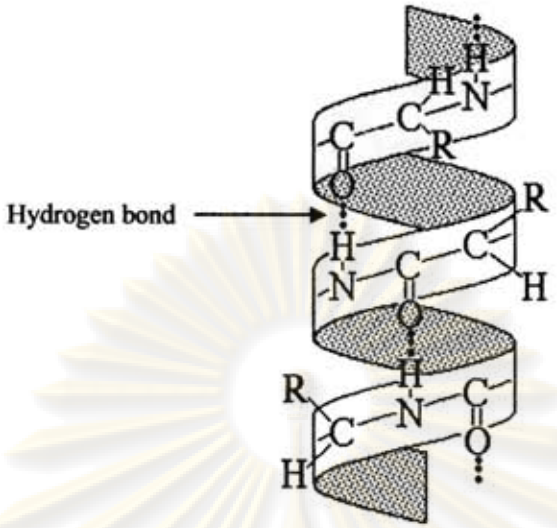

Figure 2.4 Arrangement of hydrogen bonds backbone of α-helix [28].

2.4.2.2 The β-strand

The β-strand is the second element of secondary structure. It has an extended conformation compared with the helical structure. A single β-strand is not stable because of less local stabilizing interaction. However, stable sheet-like arrangements are created when two or more β-strand form additional hydrogen bonding. Two adjacent β-strands are hydrogen bonded forming a small element of β-sheet as shown in Figure 2.5. Adjacent strands can be in parallel or antiparallel arrangements by determining the direction of the polypeptide chain from the N- to C-terminal. The two neighboring β-strand is parallel if they are aligned in the same direction from one terminus (N or C) to the other. On the other hand, it is anti-parallel if they are aligned in the opposite direction. Polyamino acid chains do not form β-sheets when dispersed in solution such that study of the formation of such structures is hindered. When strands are hydrogen bonded together to form sheets, further distortions occur especially with mixtures of parallel and anti-parallel β-strand. In general, β-sheets containing anti-parallel strand are more common than sheets made up entirely of parallel strands. Anti-parallel sheets can be formed by only two β-strands whilst at least four β-strands are required to form parallel sheets.

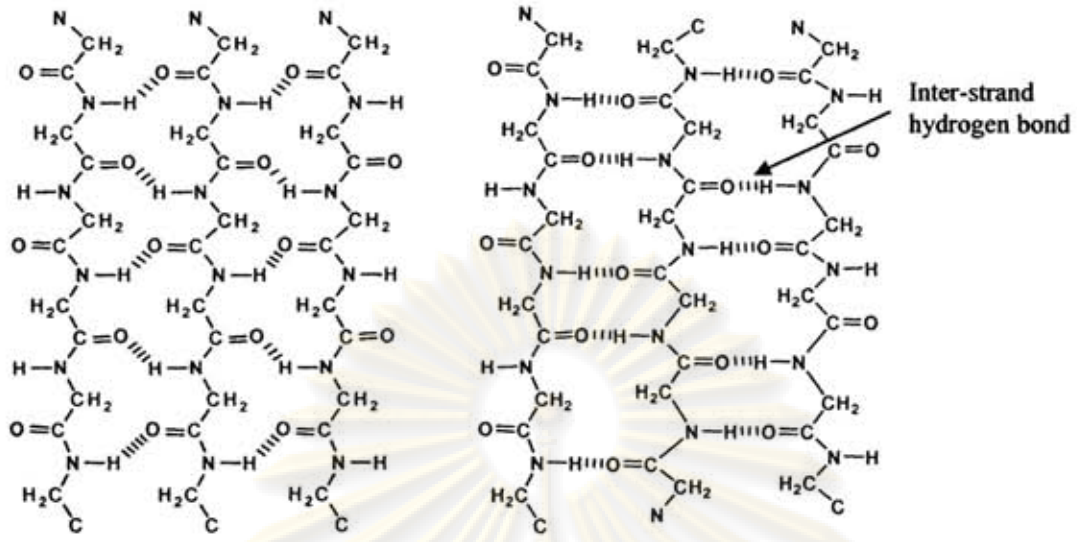

(a) Parallel β-Sheet (b) Anti-Parallel β-sheet

Figure 2.5 Two adjacent β-strands are hydrogen bonded form a small element of β-sheet forms: (a) Parallel β-sheet, and (b) Anti-Parallel β-sheet.

2.4.2.3 β-turn

A β-turn is a U-shaped, in which the polypeptide folds back nearly 180 degrees upon forming of hydrogen bonds. Hydrogen bonds are formed between the CO and NH groups of amino acid residues within the same chain as shown in Figure 2.6. The turn segment is always found to be linked to the anti-parallel β-strand. Two main types of β-turn are Type I and II which are mirror images of each other as shown in Figure 2.7.

ศูนย์วิทยทรัพยากร
จุฬาลงกรณ์มหาวิทยาลัย

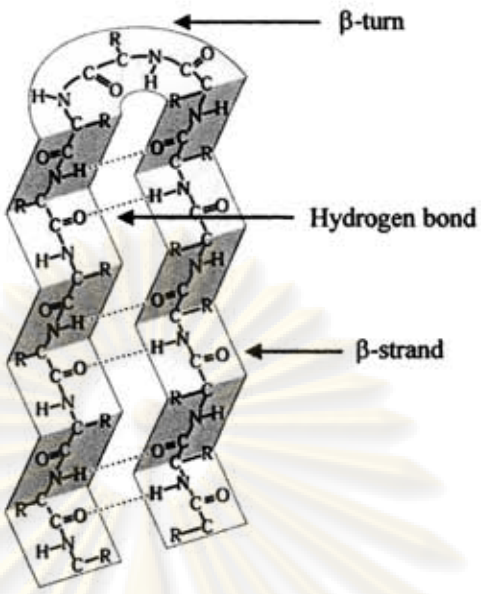

Figure 2.6 Arrangement of β-turn structure [29].

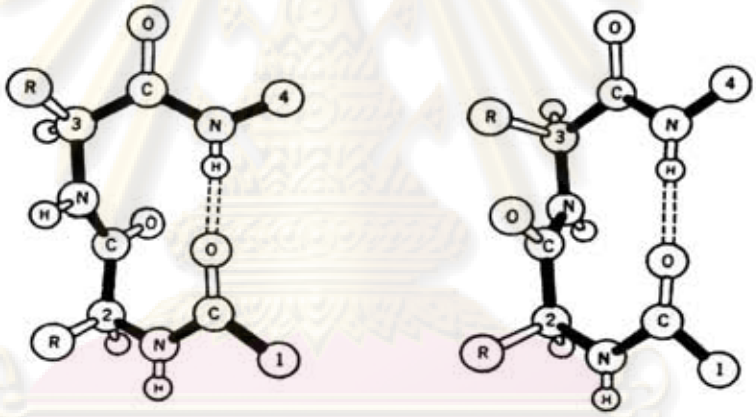

(a) Type I (b) Type II

Figure 2.7 Arrangement of atom in β-turns: (a) Type I, and (b) Type II [29].

ศูนย์วิทยทรัพยากร
จุฬาลงกรณ์มหาวิทยาลัย

2.4.2.4 Random coil

Random coil is a protein conformation where the amino acid residues are oriented randomly but still being bonded to adjacent residues as shown in Figure 2.8. It is not a specific shape, but it is a statistical distribution of shapes for all the chains in a population of macromolecules.

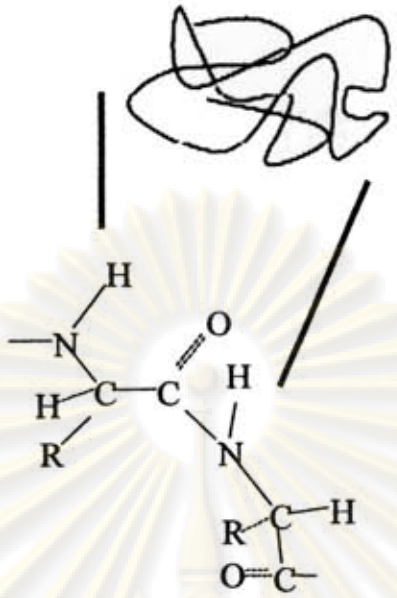

Figure 2.8 Arrangement of random coil structure.

2.4.3 Tertiary structure

Tertiary structure represents the folded-polypeptide chain that arises from the linkage of secondary structures forming a compact globular molecule. Elements of secondary structure are interacted via hydrophobic, electrostatic, van der Waals (vdW), hydrogen bonds, and also depend on the forming of disulfide (S-S) bridges [30].

2.4.4 Quaternary structure

Quaternary structure is the affiliation of two or more polypeptide chains. The interactions between these chains are exactly the same as those responsible for tertiary structure. The term "subunit" is usually used instead of polypeptide chains.

ศูนย์วิทยทรัพยากร
จุฬาลงกรณ์มหาวิทยาลัย

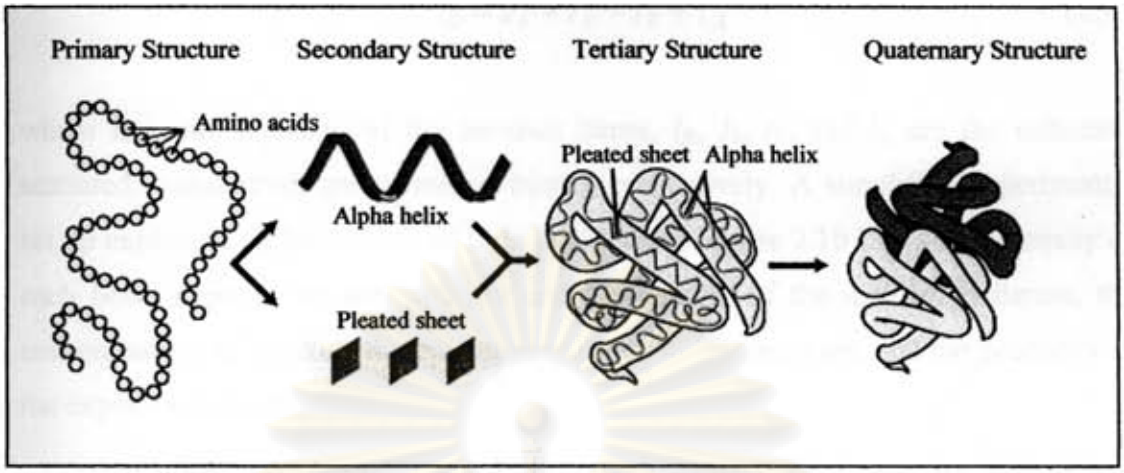

Figure 2.9 Four levels of protein structures; primary, secondary, tertiary, and quaternary structures [31].

2.5 Analysis of protein spectra to obtain secondary structural information

Researches work on proteins with many unknown characteristics. All four levels of structure are the most important features of the protein. Fourier Transform infrared (FT-IR) spectroscopy is a rapid and non-destructive technique capable of providing valuable insights into the secondary structural features in short time. Many specific subclasses of secondary structures have been resolved by correlating infrared spectra to structural information. The Amide I region is useful to study the structural features of protein because it is predominated from C=O stretching vibration of the protein backbone. However, many individual peaks are severely overlapped in this region. The methods to resolve the information are ***Fourier self-deconvolution (FSD)*** and curve fitting. Curve fitting is getting started with the estimation of the number of peaks, their locations, and their bandwidths. A predicted lineshape are typically Gaussian, Lorentzian, and also a combination of the Gaussian and Lorentzian.

2.6 Infrared spectroscopy

Spectroscopy is a scientific discipline with the electromagnetic radiation with surface sample. When electromagnetic radiation impinges on a specimen, placing between a light source and detector, the incident beam can be reflected, scattered, transmitted, or absorbed as expressed by following relationship [32].

$$I_0 = I_R + I_S + I_T + I_A \tag{2.1}$$

where I_0 is the intensity of the incident beam, I_R, I_S, I_T, and I_A are the reflected, scattered, transmitted, and absorbed beams, respectively. A simplified experimental set up explained an interaction of light is shown in Figure 2.10 [32]. The intensity of each beam depends on the intensity and wavelength of the incident radiation, the concentrations of species, the optical properties of the specimen, and the geometry of the experimental setup [32].

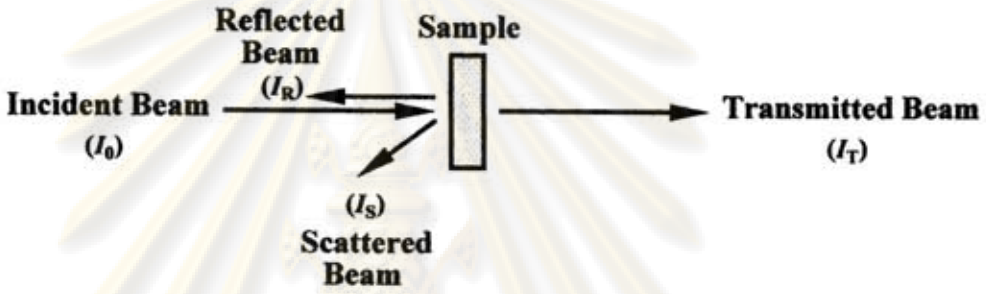

Figure 2.10 Interaction of light with matter [32].

When sample absorbs a fraction of the incident radiation, a vibration of molecules is excited. In order to measure the region and amount of light being absorbed by a sample, which is the ratio of the sample, attenuated (I) and non-attenuated (I_0) intensities of the radiation. This relationship can be quantitatively related to the chemical composition of the sample by the Beer-Lambert law as [32]:

$$I / I_0 = e^{-A(\bar{\nu})} = e^{-c_2 \varepsilon(\bar{\nu}) l} \tag{2.2}$$

where $A(\bar{\nu})$ is the absorbance at a given wavenumber $\bar{\nu}$, c_2 is the concentration of the absorbing functional group of sample, $\varepsilon(\bar{\nu})$ is the wavenumber dependent absorption coefficient, and l is the film thickness for the IR beam at a normal incidence to the sample surface.

ศูนย์วิทยทรัพยากร
จุฬาลงกรณ์มหาวิทยาลัย

2.6.1 Principles of light reflection and refraction

Refraction and reflection occur when IR beam interacts with two different media, which are different refractive index. In such a way, the beam direction is changed due to propagation velocities through two media are difference. If light propagates through an incident medium with refractive index n_1 and enters a medium with refractive index n_2, the light path will be changed and the extent of refraction is given by the following relationship.

$$n_1 \sin\alpha_1 = n_2 \sin\alpha_2 \tag{2.3}$$

where α_1 and α_2 are the angles of incidence and refraction beams, respectively.

Based on Snell's law, the principle of reflection and refraction is illustrated in Figure 2.11 [32].

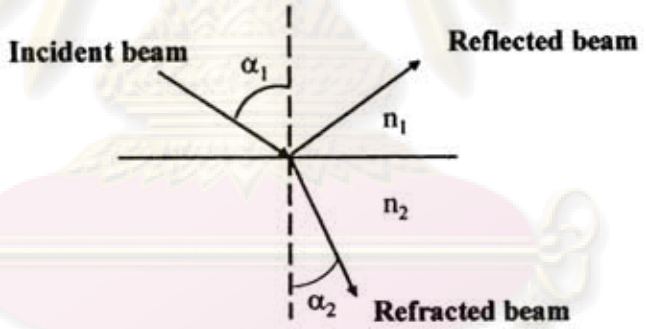

Figure 2.11 Reflection and refraction of a plane wave at a dielectric interface based on Snell's law.

2.7 Attenuated Total Reflection Fourier Transform Infrared (ATR FT-IR) Spectroscopy

ART FT-IR spectroscopy is a characterization technique based on an internal reflection phenomenon in which the radiation traveling in a higher refractive index material impinges on the interface with a less dense medium. When incident angle is

equal to the critical angle θ_c, α_2=90°, the light is totally reflected as shown in Figure 2.12. This case, all the radiation is reflected, and Snell's law can be rewritten as in Equation 2.4 [25].

$$\theta_c = \sin^{-1}(n_2 / n_1). \tag{2.4}$$

where n_2 is the lower refractive index and n_1 is the higher refractive index.

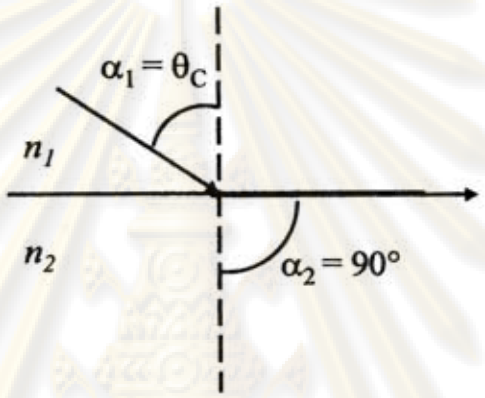

Figure 2.12 Light travels from an optically denser medium and impinges at the surface of the optically rarer medium ($n_1 > n_2$) with angle of incidence equals the critical angle.

At angles greater than critical angle, the incident radiation is completely reflected but there is an electromagnetic field that extends beyond the crystal surface, it is so-called an "***evanescent wave***". When the distance from the reflecting surface increases, the field strength is decreased. If an absorbing material is brought to contact with the IRE, the evanescent wave will be absorbed at wavelengths where the material has an absorption band. The amount of energy reflected back through the IRE will be attenuated. That is why this technique is called ***Attenuated Total Reflection***, ATR.

The distance that the evanescent wave extended passes the crystal surface and gets into any sample which contacts with this surface can be defined in terms of the depth of penetration. The depth of penetration (d_p) is defined as [32]:

$$d_p = \frac{1}{2\pi\nu n_0\left(\sin^2\theta - (n_1/n_0)^2\right)^{1/2}} \quad (2.5)$$

where ν is the frequency of the infrared radiation, n_0 is the refractive index of the IRE, n_1 is the index of refraction of the sample, and θ is the angle of incidence.

Since the electromagnetic field decreases exponentially as it moves away from the crystal surface, the sampling depth is defined as the distance from the crystal-sample interface where the intensity of the evanescent wave reduces to 1/e (~37%) of its original value. The penetration depth can be controlled either by varying the angle of incidence or selection of the IRE.

In ATR technique, the reflectivity is a measurement of the interaction of the electric field with the material and the resulting spectrum is also a characteristic of the material. The advantages of this technique are the less sample for the preparation, and the ease-of-use of internal reflection spectroscopy attachments. From the measured spectra we can obtain molecular information, chemical structure, and chemical information.

2.7.1 Internal reflection element (IRE)

Attenuated Total Reflection (ATR) occurs when a sample is brought into contact with an internal-reflection element (IRE) that has a higher refractive index than the sample. The IRE must be transparent through the mid-infrared radiation and also resist physical or chemical contact from samples. In general, the IRE configuration includes variable-angle hemispherical crystal with single reflection and multiple reflection planar crystal. The IRE is used in internal reflection spectroscopy for establishing the conditions necessary to obtain internal reflection spectra of materials (Figure 2.13). Ge is a typical IRE with a refractive index of 4.0 having significantly shallower depth of penetration than that of a ZnSe IRE with a refractive index of 2.4. Table 2.3 shows optical properties of some infrared transmitting materials [33].

Table 2.3 Information of materials used for internal reflection elements.

Material	Use of wavenumber range (cm^{-1})	Reflective index at 1000 cm^{-1}	Hardness ($kg\ mm^{-2}$)
Gemanium	5,500-600	4.02	780
Silicon	8,300-1500, 360-120	3.42	1150
Zinc selenide	20,000-460	2.43	120
Diamond	45,000-~2,500, ~1,650-200	2.417	8820

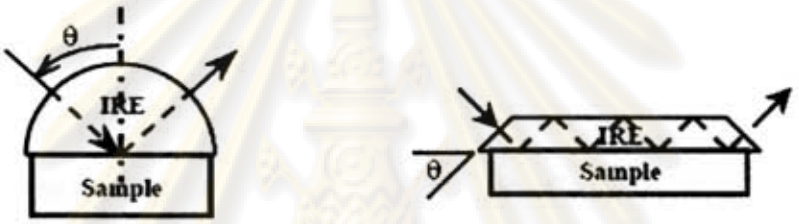

Figure 2.13 IRE configurations commonly used in ATR experimental setups: (a) Single reflection variable-angle hemispherical crystal and (b) Multiple reflection single-pass crystal.

2.7.2 Limitation of ATR FT-IR spectroscopy

ATR FT-IR spectroscopy is a surface sensitive technique. However, it has several limitations. One of them is an optical contact between the sample and IRE. The larger the air gap, the smaller the spectral intensity. If an air gap is large enough, the spectrum cannot be obtained. To solve this problem, the high pressure is applied at the sample against the IRE. Nevertheless, it has to be very carefully handled to avoid a damage of brittle IRE by an excessive pressure

2.7.3 Homemade Slide-on Ge IRE Accessory

The homemade slide-on Ge μIRE was developed by Sensor Research Unit, Department of Chemistry, Faculty of Science, Chulalongkorn University. The angle

of incidence from the objective microscope is covered the range from 15.6° to 35.5°. To eliminate interference from the internal reflection associated with the radiation having an angle of incidence smaller than the critical angle, an opaque circular adhesive tape is placed on the center of the hemispherical dome. In such manner, ATR FT-IR spectra of a small sample or a small area can be acquired.

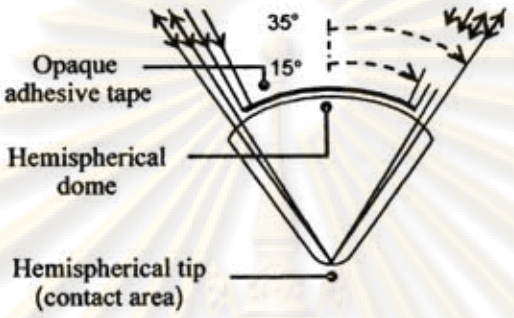

Figure 2.14 The infrared radiation tracing within the Ge μIRE.

ศูนย์วิทยทรัพยากร
จุฬาลงกรณ์มหาวิทยาลัย

CHAPTER III

EXPERIMENTAL SECTION

3.1 Materials

3.1.1 Silk fiber

Silk fiber from cocoon of *Bombyx mori*, reared locally in Queen Sirikit Sericulture (Northern Part: Phrae).

3.1.2 Chemicals

- Sodium hydrogen carbonate ($NaHCO_3$) was purchased from Fisher Scientific UK Limited, Thailand
- Citric acid ($C_6H_8O_7 \cdot H_2O$) was purchased from Merck KGAa, Thailand
- Sodium chloride (NaCl) was purchased from Carlo Erba Reagenti SpA, Thailand
- Dialysis tubing cellulose membrane, flat width 76 mm (3.0 in) (MW CO: 12,400) was purchased from Sigma-Aldrich Chemie GmbH, Thailand
- Paper filtration (Whatman ® Schleicher & Schuell, No.1), Thailand

3.1.3 Organic solvents

- Methanol was purchased from Merck KGAa, Thailand
- Ethanol was purchased from Merck KGAa, Thailand
- *iso*-propanol was purchased from Merck KGAa, Thailand

ศูนย์วิทยทรัพยากร
จุฬาลงกรณ์มหาวิทยาลัย

3.1.4 Silver nanoparticles

Silver nanoparticles were synthesized at the Sensor Research Unit (Department of Chemistry, Faculty of Science, Chulalongkorn University, Thailand) with the concentration of 50, 100, and 200 ppm.

3.2 Experimental section

3.2.1 Preparation of silk sericin microparticles

Silk sericin microparticles were obtained from the precipitation of sericin solution in organic solvents. The sericin solution was prepared by boiling silk fiber with degumming agent, such as distilled water, citric acid, and $NaHCO_3$. Sericin solution was made by dissolving 8 g of silk fiber in 1,000 mL of distilled water at 100 ° C for 8 hours. After 3 days, slurry of sericin solution was formed at room temperature; the slurry was added with distilled water and the solution of mix slurry was boiled at 100 ° C for 10 min. After the temperature decreased, the yellow sericin was formed into fibril structure and separated from sericin solution. In case of degumming with citric acid, sericin solution was prepared by dissolving 8 g of silk fiber in 1,000 mL of 1.25% (w/v) citric acid solution for 1 hour. The solution was dialyzed against distilled water for 3 days at room temperature, and pH of sericin solution was 7. The sericin solution formed into slurry during dialysis. The slurry was added with distilled water and the solution of mix slurry was boiled at 100 ° C for 10 min. After the temperature decreased, the yellow sericin formed into fibril structure and separated from sericin solution. For $NaHCO_3$ degumming, sericin solution was obtained by dissolving 8 g of silk fiber in 800 mL of 0.05% (w/v) $NaHCO_3$ solution for 1 hour. The solution was dialyzed against distilled water for 3 days at room temperature. The sericin solution is not in the slurry-form after dialysis. The sericin solution was filtered with paper filter to remove insoluble fibers. The final concentration of the sericin solution was 0.01% (w/w). Then, the sericin solutions were precipitated by organic solvents (methanol, ethanol, and *iso*-propanol) to obtain silk sericin microparticles. The volume ratio of the sericin solution to organic solvents was 1:3. Schematic illustrations of preparation silk sericin microparticles obtained from boiling solution of silk fiber by degumming agents are shown in Figure 3.1.

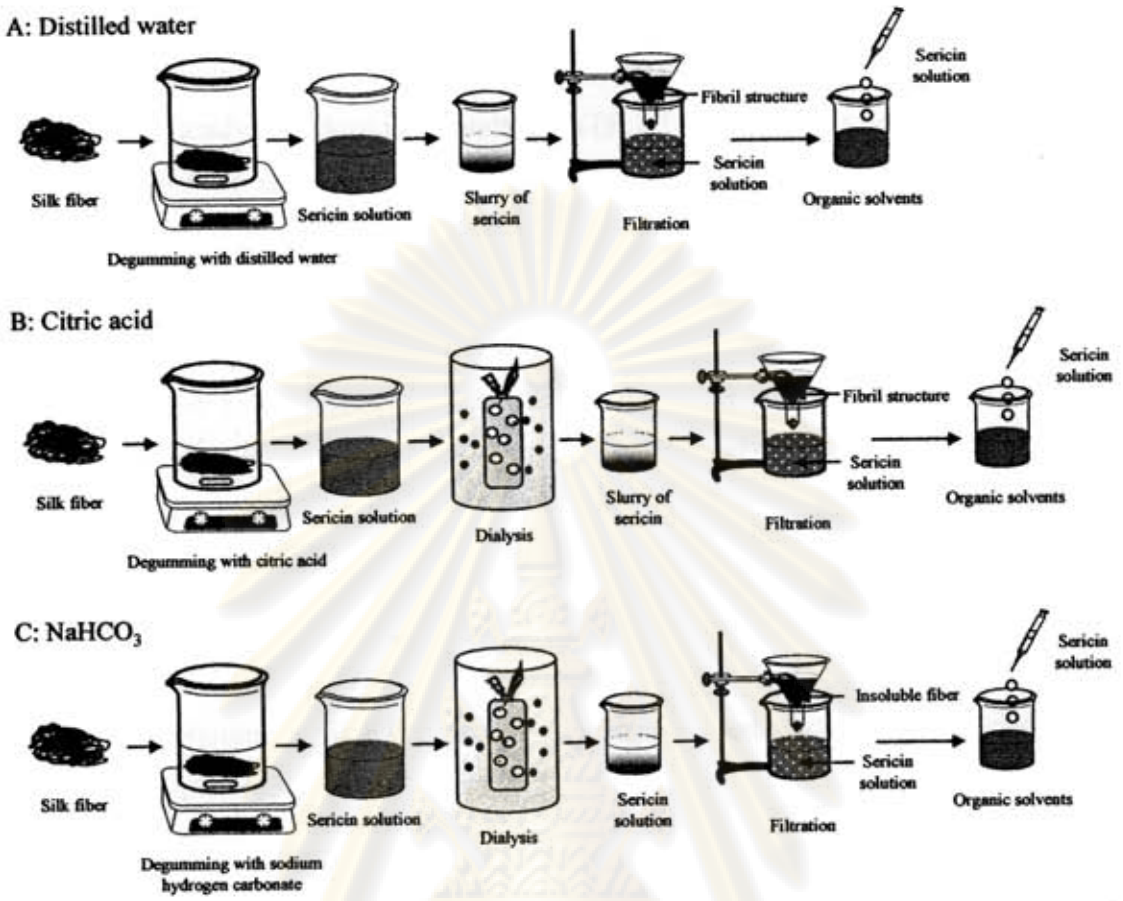

Figure 3.1 Schematic illustrations of preparation silk sericin microparticles obtained from boiling solution of silk fiber by (A) distilled water, (B) citric acid, and (C) $NaHCO_3$.

3.3 Characterization of silk sericin microparticles

3.3.1 Attenuated Total Reflection Fourier Transform Infrared (ATR FT-IR) microspectroscopy

The ATR FT-IR spectra of the sericin samples were recorded in the frequency range between 850-4000 cm^{-1} on a Nicolet 6700 FT-IR spectrometer with Continuμm™ infrared microscope equipped with a mercury-cadmium-tellurium (MCT) detector at resolution of 4 cm^{-1}. All samples and backgrounds were collected at 128 co-addition times. ATR measurements were performed by means of homemade slide-on germanium (Ge) μIRE. Samples were placed on the glass slide and dried by

heating. Then, the glass slide was fixed on the microscope stage. The ATR spectra of samples were acquired in the reflection mode under infrared microscope. The schematic diagram of the ATR measurement is shown in Figure 3.2.

Prior to analyzing Amide I bands of ATR FT-IR spectra, a baseline correction was performed at around 1740 and 1580 cm^{-1}. Second derivative spectra were calculated to identify the positions of the overlapping component bands in the Amide I region, which were used as initial parameters for curve fitting analysis [3]. Self-deconvolution was also performed to determine the peak frequency to ensure the fidelity of each method [34]. The secondary structural information in the Amide I region between 1740-1580 cm^{-1} was fitted with Gaussian/Lorentzian function. The fitted band areas were used to calculate the proportion of the secondary structures.

Instrument

1. Nicolet 6700 FT-IR spectrometer equipped with a mercury-cadmium-telluride (MCT) detector.
2. Continuμm™ infrared microscope with 15X Cassegrain infrared objective and 10X glass objective.
3. Homemade slide-on germanium (Ge) μIRE

ศูนย์วิทยทรัพยากร
จุฬาลงกรณ์มหาวิทยาลัย

Default Spectral Acquisition Parameter

Nicolet 6700 FT-IR Spectrometer

Instrumental Setup

Source	Standard Globar™ Infrared Light Source
Detector	MCT
Beam splitter	Ge-coated KBr

Acquisition Parameters

Spectral resolution	4 cm^{-1}
Number of scans	128 scans
Spectral format	Absorbance
Mid-infrared range	4000-650 cm^{-1}

Advanced Parameters

Zero filing	none
Apodization	Happ-Genzel
Phase correction	Mertz

Continuμm™ Infrared Microscope

Instrumental Setup

Detector	MCT
Objective	15X Schwarazschild-Cassegrain
Aperture size	150 μm x 150 μm

ศูนย์วิทยทรัพยากร
จุฬาลงกรณ์มหาวิทยาลัย

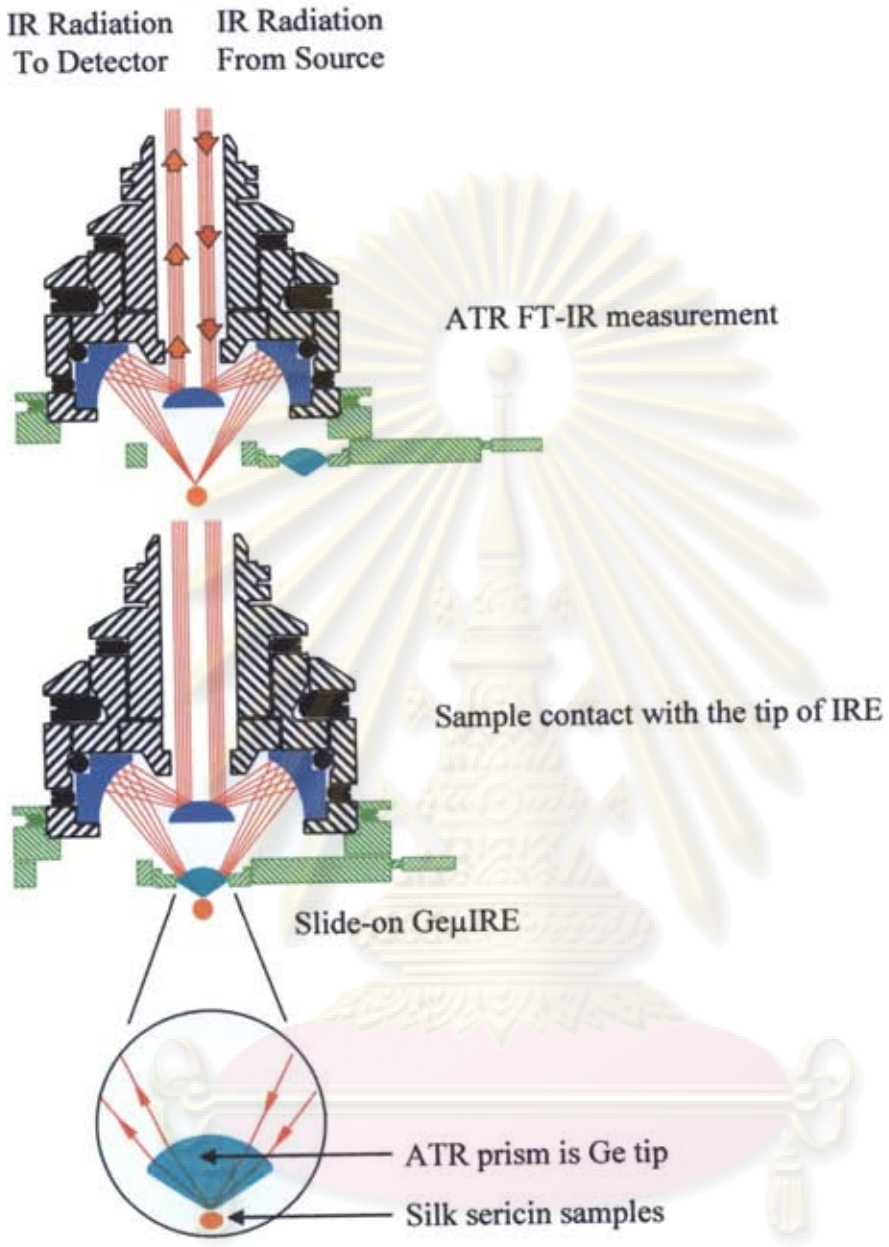

Figure 3.2 Schematic diagram of ATR measurement configuration.

ศูนย์วิทยทรัพยากร
จุฬาลงกรณ์มหาวิทยาลัย

Figure 3.3 ATR FT-IR microspectroscope: (A) Continuμm® infrared microscope coupled with the Nicolet 6700 FT-IR spectrometer, (B) the slide-on Ge μIRE is fixed on the position of slide-on housing on the infrared objective, and (C) Homemade slide-on germanium (Ge) μIRE.

3.3.2 Scanning electron microscope (SEM)

The morphology of the silk sericin microparticles was observed by scanning electron microscope (SEM) of JEOL, JSM-6480LV model shown in Figure 3.4. One drop of the particle suspension was placed on a glass slide. After air drying, the sample was coated with gold by an ion sputter and observed at 15 kV accelerating voltage.

Figure 3.4 Scanning electron microscope (SEM).

ศูนย์วิทยทรัพยากร
จุฬาลงกรณ์มหาวิทยาลัย

3.4 The deposit of silver nanoparticles on silk sericin microparticles

Silk sericin microparticles were centrifuged at 1500×g for 15 minutes to separate from methanol. The distilled water was added to silk sericin microparticles, after that the silk sericin microparticles suspended in distillated water twice with Vortex Genie. The final volume of silk sericin microparticles suspended in distillated water is 2 mL. They were added with 10 mL of silver nanoparticles at different concentration in silk sericin microparticles suspended in distilled water. The investigation of the deposition of silver nanoparticles at different concentration (50 ppm, 100 ppm, and 200 ppm) onto silk sericin microparticles was performed. The mixture was ultrasonicated until they were homogeneously mixed and maintained at room temperature. After 3 days, silk sericin microparticles were precipitated again. The concentrations of silver nanoparticles in supernatant were measured by UV-visible spectrometer. The observed molecular conformation of silk sericin microparticles after adding silver nanoparticles were monitored by ATR FT-IR microspectroscopy. The morphology of silver nanoparticles deposited on the silk sericin microparticles were investigated by transmission electron microscope (TEM).

3.4.1 UV-visible spectroscopy

UV-visible spectroscopy was utilized to determine the amount of silver nanoparticles deposited on silk sericin microparticles. The differences of maxima absorption of silver nanoparticles before and after deposition of silver nanoparticles on silk sericin microparticles were measured. Before collecting the spectrum, a reference of distilled water is collected. If the absorbance of the sample was too high for collecting the spectrum, the samples were 20 times diluted with distilled water. The instrument setup was shown in Fig. 3.5.

ศูนย์วิทยทรัพยากร
จุฬาลงกรณ์มหาวิทยาลัย

Instrument Setup

Model	USB 4000
Source	Deuterium-Halogen light source DH 2000
Wavelength range	UV-Vis-NIR
Detector	Toshiba TCD 1304 AP, 3648-element linear silicon CCD array
Grating	600 Line Blazed at 300 nm
Bandwidth	200-850 nm

Spectra Acquisition Parameter

Software	Ocean Optics Inc. Spectra Suit
Integration time	10 milliseconds
Scans to Average	128 scans
Box car width	10 nm
Spectra format	Absorbance
Spectra range	200-850 nm

Figure 3.5 UV-Visible spectrometer.

3.4.2 Transmission electron microscope (TEM)

The morphology and particles size of silver nanoparticles deposited on silk sericin microparticles was characterized by TEM. The TEM images were performed on Hitashi H-7650 (Hi-Technologies Corporation) at an accelerating voltage of 100 kV (as shown in Figure 3.6). One drop of the silver-nanoparticles-coated-silk sericin microparticles was placed on a copper grid. The grid was allowed to dry for 1 day. Then the images of silver nanoparticles deposited on silk sericin microparticles were collected.

Figure 3.6 Hitashi H-7650 transmission electron microscope.

ศูนย์วิทยทรัพยากร
จุฬาลงกรณ์มหาวิทยาลัย

CHAPTER IV

RESULTS AND DISCUSSION

4.1 Silk sericin microparticles

To prepare sericin solution from boiling silk fiber; distilled water, citric acid, and $NaHCO_3$ were used as degumming agent. Consequently, silk sericin microparticles were obtained by precipitating the sericin solution in organic solvents (e.g. methanol, ethanol, and *iso*-propanol). The morphology of silk sericin microparticles were observed by scanning electron microscope (SEM). The molecular conformation of native silk sericin and silk sericin microparticles has been investigated by means of ATR FT-IR spectroscopy. Figure 4.1 shows the images of silk sericin microparticles obtained from boiling sericin solution of silk fiber with different degumming agent, and further treated with different organic solvents. By using distilled water and citric acid as degumming agent, the obtained sericin solution were in slurry forms at room temperature. Subsequently, an agglomeration is formed due to high molecular weight of the sericin peptide [26]. Distilled water was added into the slurry, and it was boiled till completely dissolved. Afterward, the temperature of solution was decreased. Formation of the yellow sericin to fibril structure occurred and was separated from sericin solution. The yellow fibril structure was removed and the sericin solution was further precipitated in organic solvents. The obtained sericin solution was not in slurry form when used $NaHCO_3$ as degumming agent. This due to the fact that $NaHCO_3$ can degrade polypeptides into amino acid. With different degumming agents, the observed images of silk sericin microparticles are obviously dissimilar, Figure 4.1. Sericin solution is yellow when degumming with $NaHCO_3$. The solutions are colorless when degumming with distilled water and citric acid. The color of sericin solution is also consistent with that of its microparticles.

Figure 4.1 Silk sericin microparticles obtained from solution of silk fiber degumming with (A) distilled water, (B) citric acid, and (C) $NaHCO_3$ after treating with organic solvents: (a) methanol, (b) ethanol, and (c) *iso*-propanol.

4.2 The Morphology of native silk sericin and silk sericin microparticles

Morphology of native and microparticles of silk sericin has been investigated by scanning electron microscope (SEM). SEM images of silk sericin microparticles at different preparative conditions in comparison with the images of native structure are shown in Figure 4.2. The SEM images of native silk sericin were taken at three different positions. The particle sizes of silk sericin microparticles were in the range of micro-scale but it does not completely isolate. The particles size of silk sericin is distributed from 3-8 μm with an average particle size of about 5 μm (Table 4.1).

ศูนย์วิทยทรัพยากร
จุฬาลงกรณ์มหาวิทยาลัย

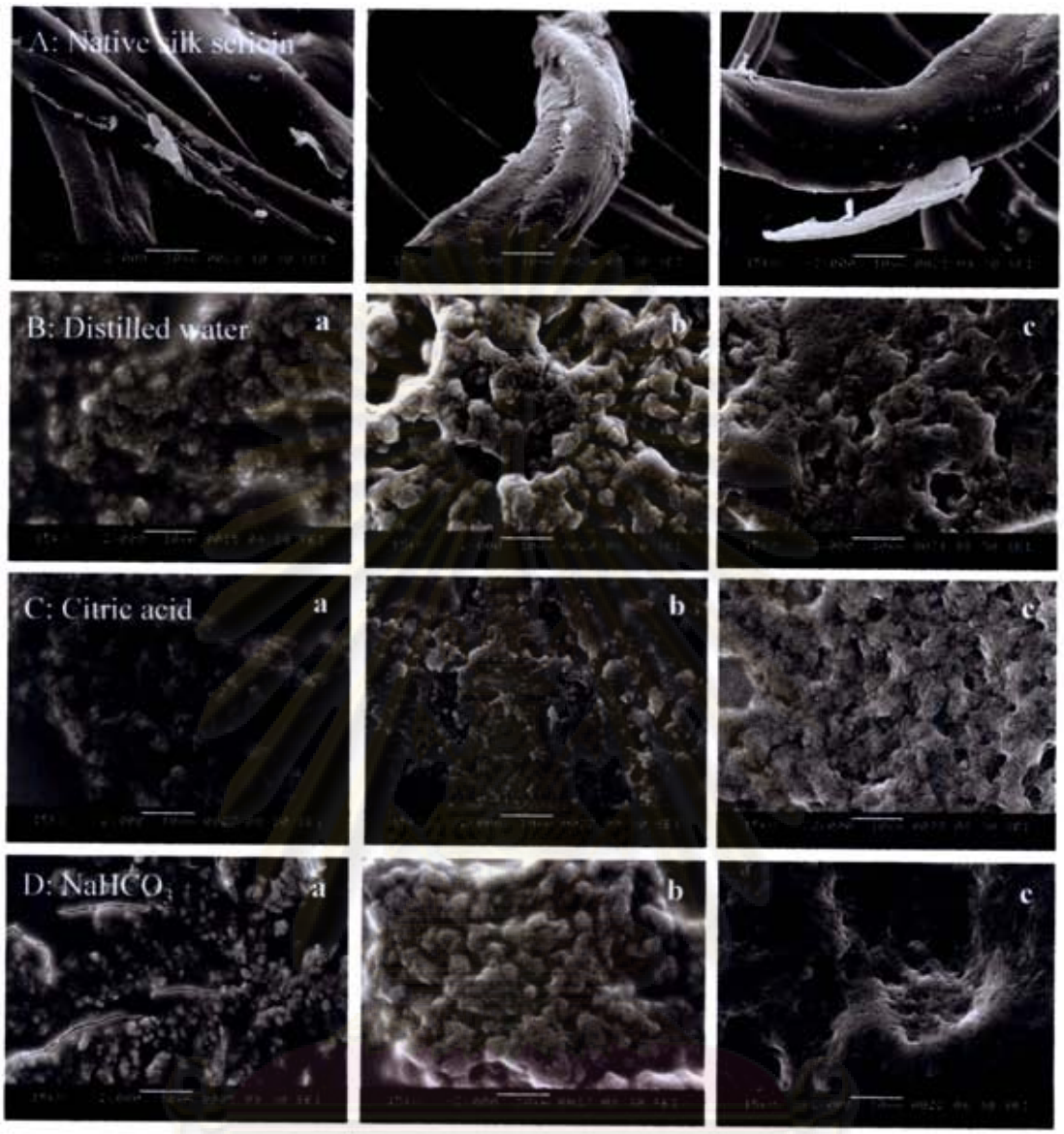

Figure 4.2 SEM images of (A) native silk sericin at three different positions, silk sericin microparticles obtained by precipitating of sericin solution boiled with (B) distilled water, (C) citric acid, and (D) $NaHCO_3$ in organic solvents: (a) methanol, (b) ethanol, and (c) *iso*-propanol.

ศูนย์วิทยทรัพยากร
จุฬาลงกรณ์มหาวิทยาลัย

Table 4.1 Particles size of silk sericin microparticles.

Sericin solution prepared from boiling of silk fiber with degumming agent	Particles size (μm) of silk sericin microparticles treated with organic solvents		
	methanol	ethanol	*iso*-propanol
Distilled water	3.96±0.20	7.16±0.40	7.95±0.65
Citric acid	4.84±0.18	4.54±0.21	5.16±0.18
$NaHCO_3$	3.30±0.27	6.11±0.34	7.83±0.61

4.3 ATR FT-IR spectra of native silk sericin

Figure 4.3 shows the ATR FT-IR spectrum of native silk sericin. At three different positions of the same sample, the patterns of absolute spectra are the same, (Figure 4.4). After normalized to Amide I band at 1620 cm^{-1}, the spectra are superimposed. This implied that the homemade slide-on Ge μIRE has a very high efficiency with reproducible measurement. Similarity of the absorbance spectra indicates the same chemical structure for the whole native silk sericin.

4.4 Structural information of native silk sericin

The native silk sericin composes of protein, water, lipid, and wax. A broad band centered at 3273 cm^{-1} is attributed to N-H stretching vibration of amide groups and O-H stretching vibration of hydroxyl amino acid residues. However, an abundance of serine and threonine residues cause a difficulty on obtaining structural information from N-H stretching vibration because is its absorption band overlapped with a strong O-H stretching at 3500-3200 cm^{-1}. The predominant absorption bands at 1620, 1515, and 1235 cm^{-1} are Amide I, II, and III vibrational frequencies, respectively. Amide I band primarily represents a C=O stretching vibration of the amide group. Amide II band contains a contributions of N-H bending and C-N stretching vibrations. In the Amide III region, an information of N-H bending plus C-N stretching and a contribution of O=C-N bending are obtained.

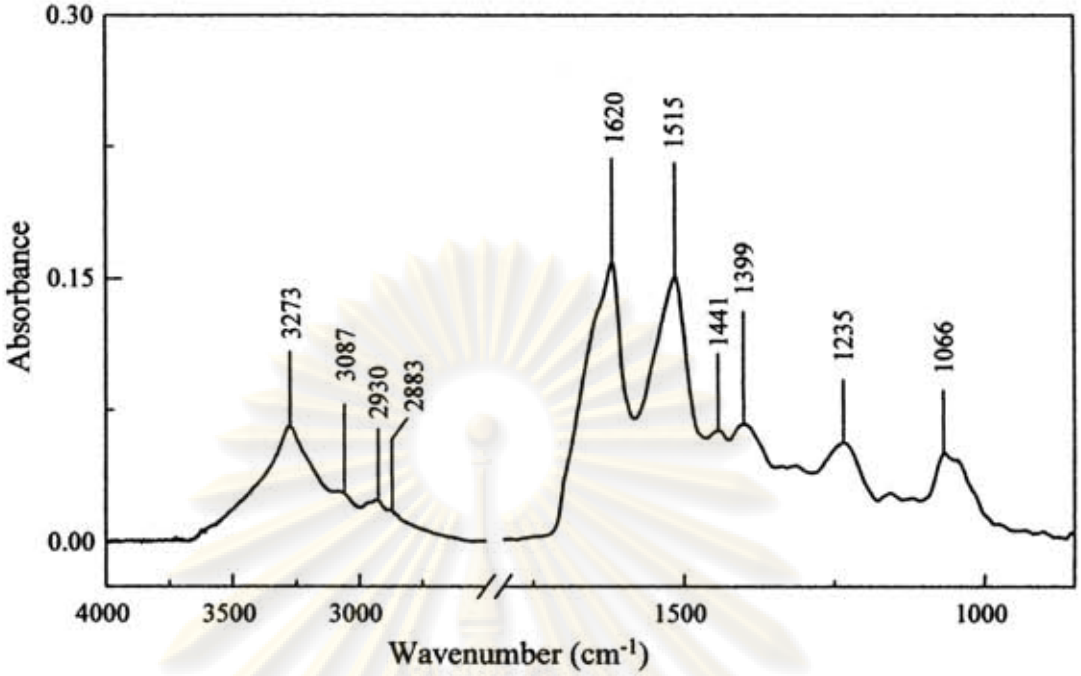

Figure 4.3 ATR FT-IR spectrum of native silk sericin.

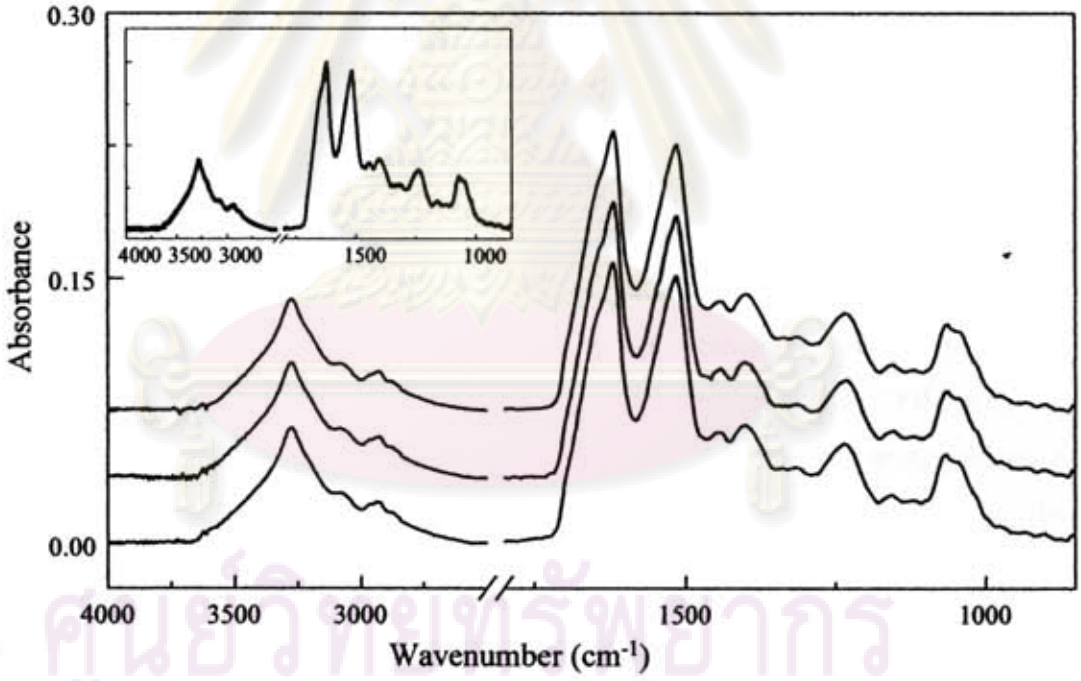

Figure 4.4 ATR FT-IR spectra of native silk sericin from a single silk fiber collected at three different positions. The inset is the normalized spectra.

4.5 ATR FT-IR spectra of native silk sericin and silk fibroin fiber

Figure 4.5 shows the ATR FT-IR spectra of native silk sericin and silk fibroin fiber, which are significantly different. The band at 3273 cm^{-1} of the native silk sericin is broader than that of silk fibroin fiber. This because silk sericin is a highly hydrophilic protein [19] and its can absorb more water. From these results, it can be concluded that the native silk sericin is more moisture in its structure than that of silk fibroin fiber. The Amide I band of the silk sericin is centered at 1618 cm^{-1}, which is 5 cm^{-1} lower than that of fibroin fiber. It has been assigned to aggregate β-strands segments, which may be related to an abundance of polar side chains such as hydroxyl and carboxyl groups. These side chains can form intermolecular hydrogen bonds with other polar side chains or amide groups in peptide backbones. Moreover, the Amide I band of silk sericin is broader than that of the silk fibroin fiber indicated more random coil structure for the silk sericin. Another Amide I band at 1623 cm^{-1} of silk fibroin fiber together with a shoulder at higher frequency (1696 cm^{-1}) has been assigned to antiparallel β-sheet. Amide II bands of silk sericin and silk fibroin fiber are centered at about the same frequencies. Amide III band of silk sericin is boarder (1235 cm^{-1}) than that of silk fibroin (1262 and 1230 cm^{-1}). The difference of peak frequencies of both spectra can be related to the different amino acid composition between silk fibroin and native silk sericin. Particularly the bands at 1399 and 1066 cm^{-1} are more intense in the spectrum of sericin because it has the poly-serine in the structure. These peaks can be attributed to C-H/O-H bending and C-OH stretching vibrations, respectively. It was already known that the amino acid compositions of native silk sericin and silk fibroin fiber are different, in which the silk fibroin fiber contains a greater amount of alanine and glycine than that of the native silk sericin. Moreover, the spectrum of sericin lacks the bands at 998 and 976 cm^{-1}, which are typically assigned to Gly-Ala sequences in silk fibroin fiber [35]. The summary of peak assignments is in Table 4.2.

ศูนย์วิทยทรัพยากร
จุฬาลงกรณ์มหาวิทยาลัย

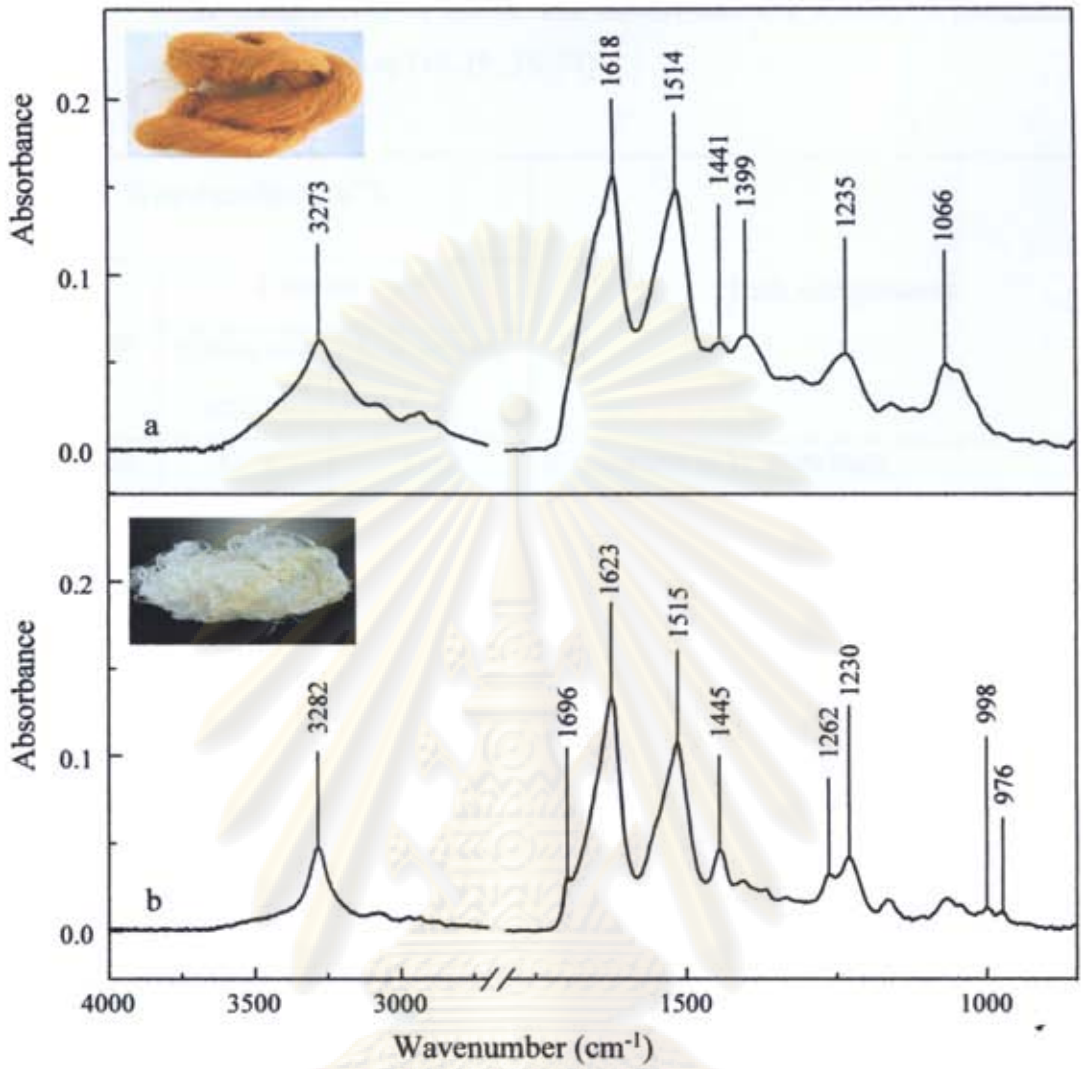

Figure 4.5 ATR FT-IR spectra of (a) native silk sericin and (b) silk fibroin fiber.

ศูนย์วิทยทรัพยากร
จุฬาลงกรณ์มหาวิทยาลัย

Table 4.2 Peak assignments of native silk sericin and silk fibroin in comparison with the literatures [18-19, 35-37].

Wavenumber (cm^{-1})			Peak assignments
Literatures	Current work		
	Native silk sericin	Silk fibroin fiber	
3385-3160	3273	3282	Symmetric N-H stretching
3100-3070	3087	3078	Overtone of Amide II
2975-2950	-	2973	Asymmetric C-H stretching of CH_3
2940-2915	2936	2931	Symmetric C-H stretching of CH_3
2885-2865	2883	-	Asymmetric C-H stretching of CH_2
1703-1697	-	1696	Antiparallel β-sheet
1700-1600	1620	1623	Amide I C=O stretching
1580-1510	1515	1514	Amide II N-H bending (wagging) plus C-N stretching
1480-1440	1441	1445	C-H bending (scissoring) of CH_2
1410-1350	-	1407	C-H bending (wagging) of CH_3
1440-1260	1399	-	C-H and O-H bending vibration
1305-1200	1235	1262,1230	Amide III N-H bending (twisting) plus C-N stretching and contribution from O=C-N bending
1090-1000	1066	-	C-OH stretching vibration
1175-1165	-	1166	O-H bending of phenolic residue in Tyr
1100-1050	-	1069	C-N stretching of RCH_2-NH_2, R_2CH-NH_2
1060-900	-	998, 976	C-C skeletal of Gly-Ala sequences

4.6 Secondary structure of native silk sericin and silk fibroin fiber analyzed by ATR FT-IR spectroscopy

Protein generally contains more than one secondary structure, which are correlated to the amide groups of protein spectra. Most of secondary structure of

protein can be classified as α-helix, β-sheet, β-turns, and random coil. Analysis of secondary structure of protein by means of FT-IR spectroscopy is an established technique. Since secondary structures are associated with a characteristic pattern of hydrogen bonding between amide C=O and N-H groups. Amide I absorption found in the 1700-1600 cm^{-1} region is the most useful evidence for determining protein secondary structures. The Amide I band was used to monitor the structural change of protein because it is predominantly from C=O stretching vibration of the protein backbone [19].

However, overlapping of the bands in this region is an obstacle to extract the information of secondary structure. The second derivative and deconvolved method have been applied to distinguish the overlapped peaks [38-40]. The peak positions of native silk sericin and silk fibroin fiber were determined from second derivative and deconvolved spectra, the curve fitting was applied to determine the proportions of secondary structures in protein, as shown in Figure 4.6. Absorption centers of curve fitting of silk sericin and silk fibroin are shown in Table 4.3. The absorption peaks in the region 1622-1627 cm^{-1} are attributed to antiparallel β-sheet [38]. Silk fibroin fiber exhibits a strong Amide I band at 1622 cm^{-1}, which is not found in the spectrum of silk sericin, is assigned to antiparallel β-sheet (intermolecular). A small shoulder at 1698 cm^{-1} is also assigned to the same segment. The other peak positions located at 1646, 1657, and 1679 cm^{-1} have been assigned to random coil, α-helix and β-turn, respectively. Silk sericin contains the aggregate β-strands as represented by the peak at 1617 cm^{-1}, which is not observed for silk fibroin. The band at 1632 cm^{-1} is also only found in the spectrum of silk sericin, it is assigned to β-sheet (intramolecular). The bands at 1646, 1662, and 1680 cm^{-1} of silk sericin are assigned to random coil, α-helix and β-turn, respectively. These peaks are slightly shifted from those observed for silk fibroin, which might be due to the difference of hydrogen bonding of protein. The proportions of each secondary structure were estimated from the component bands by integrating the peak area; Table 4.4. Aggregate β-strands (33.90%) is populated in silk sericin, and silk fibroin is populated by β-sheet element (44.81%). Silk sericin has more random coil structure (24.29%) than that of silk fibroin (19.89%). Similarly, helical structure (20.53%) is more favorable in silk sericin. The information of these secondary structures indicates a less crystalline structure of the silk sericin compared to that of silk fibroin fiber.

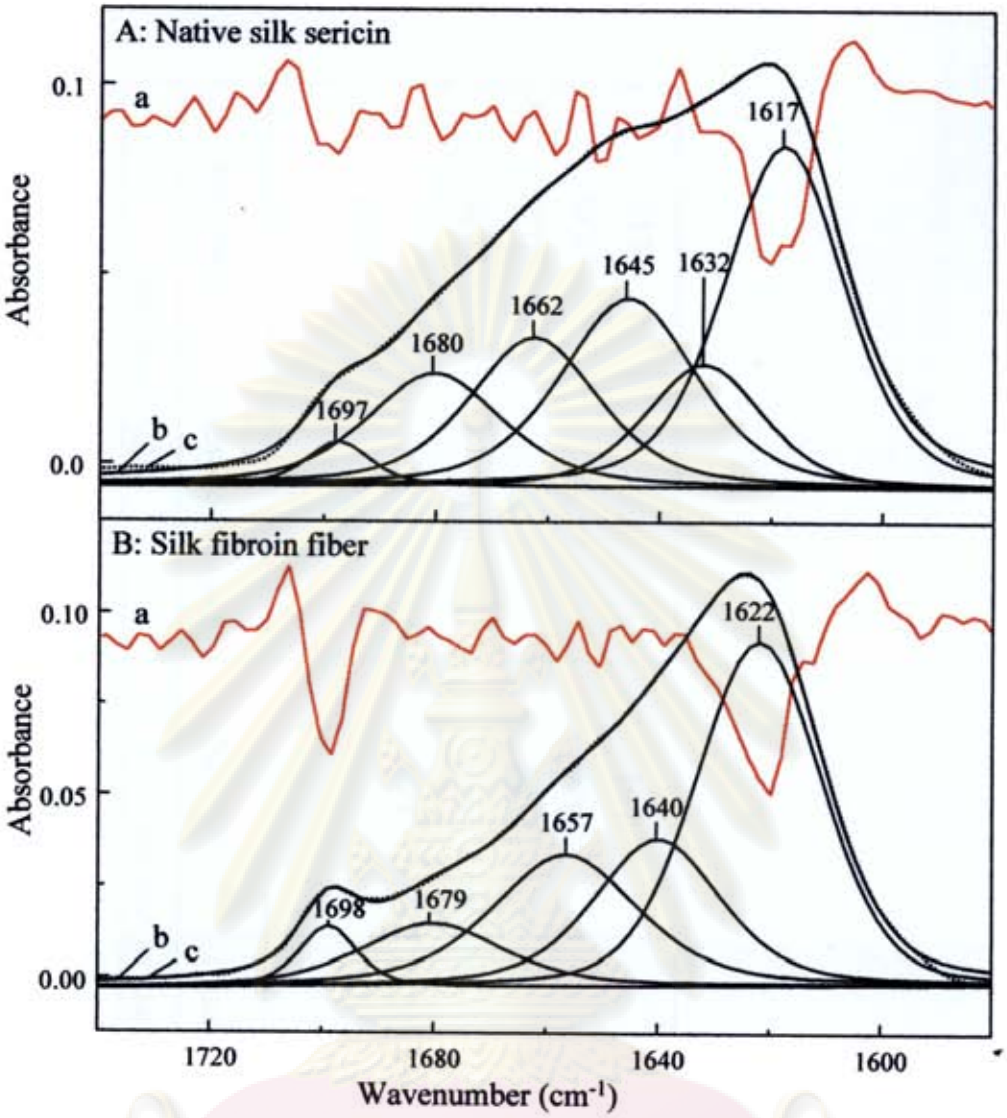

Figure 4.6 Curve fitting of (A) native silk sericin, and (B) silk fibroin fiber spectra in the Amide I region: (a) second derivative spectrum, (b) deconvolved (solid line) spectrum, and (c) original (dotted line) spectrum.

ศูนย์วิทยทรัพยากร
จุฬาลงกรณ์มหาวิทยาลัย

Table 4.3 Carbonyl absorption associated with the secondary structure of native silk sericin and silk fibroin [16, 19, 41].

Literatures	Assignments	Current work			
		Native silk sericin		Silk fibroin fiber	
		Wavenumber (cm^{-1})	Area (%)	Wavenumber (cm^{-1})	Area (%)
1605-1621	Aggregate β-strand	1617	33.90	-	-
1622-1627	β-sheets (Intermolecular)	-	-	1622	44.81
1628-1637	β-sheets (Intramolecular)	1632	11.54	-	-
1638-1655	Random coil	1646	24.29	1640	19.89
1656-1662	α-helix	1662	16.67	1657	20.53
1663-1696	β-turn	1680	10.69	1679	10.60
1697-1703	β-sheets (Intermolecular)	1697	2.91	1698	4.17

ศูนย์วิทยทรัพยากร
จุฬาลงกรณ์มหาวิทยาลัย

4.7 Characterization of silk sericin solution and silk sericin microparticles

4.7.1 ATR FT-IR spectra of slurry, sericin solution, and yellow fibril sericin

Degumming with citric acid, the sericin solution has the same property as that obtained by degumming with distilled water. The obtained silk sericin solutions were separated into two proportions, which are called ***"sericin solution"*** and ***"yellow fibril sericin"***, in dialyzed bag. Some scientists defined these two proportions as α- and β-sericin, respectively [42]. The α-sericin in the boiling water is more soluble than the β-sericin [43]. Moreover α-sericin has more N and O than the β-sericin, but the β-sericin has more C and H than the α-sericin [42]. The Amide I band of yellow fibril sericin, degumming with distilled water and citric acid, is centered at 1620 cm^{-1} which is typically representative to aggregated strands, see Figure 4.7 (A and B). Formation of β-strand aggregates prevents its molecule to be dissolute in water [44]. Polypeptide chains containing hydroxyl side chain in disordered structure is become mobile upon hydration, which may transform into the more stable form as β-sheet aggregates. The Amide I band of the slurry and sericin solution is exhibited at 1638 cm^{-1}, which has been assigned to random coil structure. The slurry and sericin solution are soluble protein, which consists of disorder structure. The band at 1441 cm^{-1} is more intense in the spectra of fibril sericin. This band is attributed to C-H bending vibration of CH_2, which is consistent with the previous report that fibril sericin is more populated with C and H than sericin solution. The sericin solution is more soluble than yellow fibril sericin in water. It is found that the sericin solution is amorphous while yellow fibril sericin is the aggregate β-strand. In this research, the yellow fibril sericin was removed from sericin solution and sericin solution is further utilized to prepare silk sericin microparticles. On the contrary, the obtained sericin solution upon degumming with $NaHCO_3$ is not in slurry form, and it does not precipitate in organic solvents for forming the micro-structure. Therefore, the solution must be added with NaCl in order to initiate the precipitation. In this research, the lowest concentration of 0.05% (w/v) NaCl was added to prepare sericin microparticles by precipitating sericin solution in organic solvents. Ions are classified as ***kosmotropic*** or ***chaotropic***, based on their size and charge [45]. Na^+ is weakly kosmotropic and Cl^-

is weakly chaotropic [46]. Kosmotropic ions strongly interact with oppositely charges residues on the protein surface due to their high charge density [46]. ATR FT-IR spectra of sericin solution before and after adding NaCl are similar, as shown in Figure 4.7 (C). Amide I band of both spectra is exhibited at 1643 cm^{-1} which is typically representative to random coil structure.

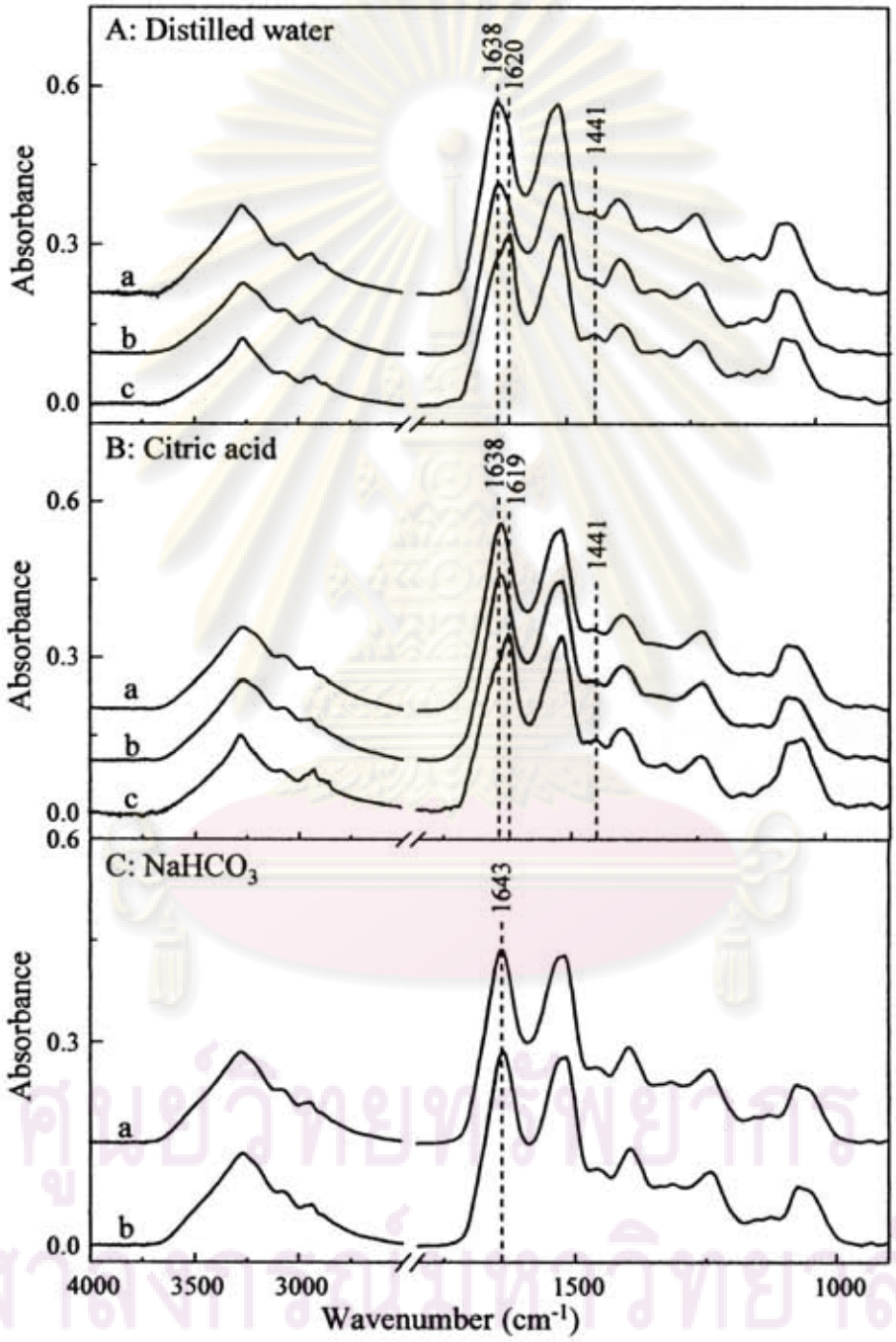

Figure 4.7 ATR FT-IR spectra of silk sericin degumming with (A) distilled water, and (B) citric acid: (a) slurry, (b) sericin solution, and (c) yellow fibril sericin; ATR FT-IR spectra of sericin degumming with (C) $NaHCO_3$: (a) sericin solution and (b) sericin solution after adding NaCl.

4.7.2 ATR FT-IR spectra of silk sericin microparticles

When sericin solution is mixed with organic solvents which are less polarity than water, it tends to be less soluble. In such a way, a new technique for the preparation of silk sericin microparticles is developed by precipitation of sericin solution in organic solvents. The ATR FT-IR spectra of silk sericin microparticles are shown in Figure 4.8, the characteristic absorption bands are observed at 1618 cm^{-1} (Amide I), 1515 cm^{-1} (Amide II), and 1238 cm^{-1} (Amide III). The Amide I bands of sericin microparticles obtained by precipitating sericin solution in different organic solvents are compared; sericin microparticles treated with methanol has the sharpest band. The Amide I band is broader when precipitated in ethanol and *iso*-propanol, respectively. Upon precipitating of sericin solution in organic solvents, hydrogen bonds among sericin chains is become stronger because of the hydrophobicity of organic solvents encouraging the formation of aggregated β-strand. Strong interchain interaction may be related to the abundance of polar side chains such as hydroxyl and carboxyl groups which can form interchain hydrogen bonds with other polar side chains or amide groups in peptide backbones. According to the Amide I band of the sericin microparticles; methanol is more effective than ethanol and *iso*-propanol for the induction of structural changes from random coil to β-sheet. This means sericin microparticles treated with methanol have the most β-sheet-rich structure. On the contrary, sericin solutions obtained from degumming solution with $NaHCO_3$ cannot prepare silk sericin microparticle form by precipitation solution in organic solvent. Therefore, NaCl was added. Amide I bands of sericin microparticles are observed at 1639 cm^{-1} (Amide I), 1517 cm^{-1} (Amide II), and 1242 cm^{-1} (Amide III). These bands are slightly shifted from those observed in the spectra of microparticles after degumming with distilled water and citric acid. Amide I bands of sericin microparticles obtained by precipitating of sericin solution treated with different organic solvents (methanol, ethanol and *iso*-propanol) are about the same. As one can say, silk sericin microparticles obtained by precipitating of sericin solution in organic solvents do not change from random coil to β-sheet if $NaHCO_3$ was used as degumming agent. The spectra of sericin microparticles obtained by precipitating sericin solution degummed with $NaHCO_3$ differ from those obtained after degumming

with distilled water and citric acid. The functional groups associated with each absorptions band and the other functional groups are summarized in Table. 4.4.

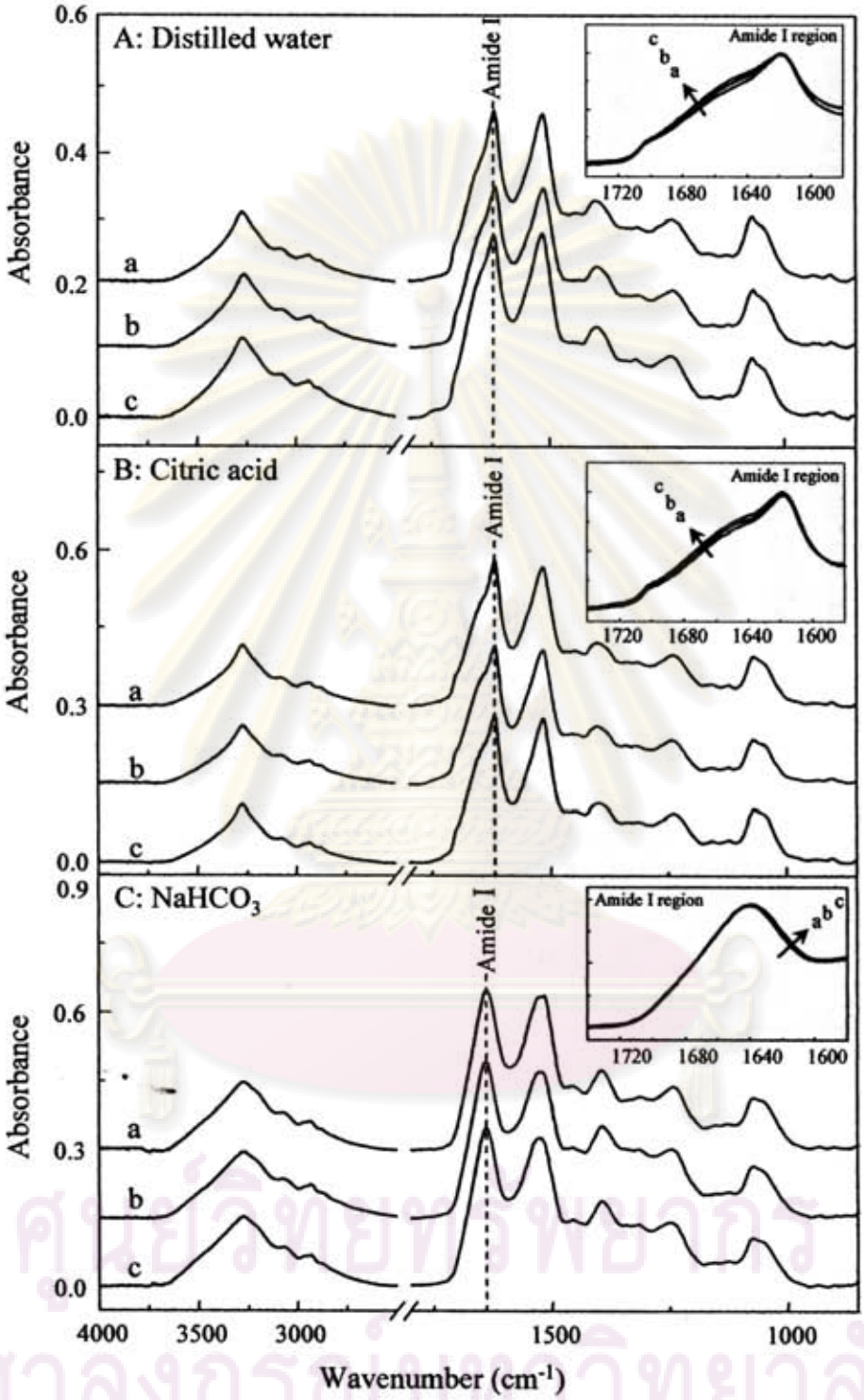

Figure 4.8 ATR FT-IR spectra of sericin microparticles obtained from boiling solution of silk fiber with (A) distilled water, (B) citric acid, and (C) $NaHCO_3$ treated with different organic solvents: (a) methanol, (b) ethanol, and (c) *iso*-propanol. The inset is the normalized spectra in Amide I region.

Table 4.4 Peak assignments of silk sericin microparticles [16, 19, 35-36].

Literatures	Wavenumber (cm^{-1})									Peak assignments
	Sericin solution obtained from boiling of silk fiber with degumming agent									
	Distilled water			Citric acid			$NaHCO_3$			
	Silk sericin microparticles treated with									
	me	et	*iso-*	me	et	*iso-*	me	et	*iso-*	
3385-3160	3275	3272	3274	3272	3271	3277	3271	3268	3280	Symmetric N-H stretching
3100-3070	3090	3080	3088	3087	3087	3088	3077	3075	3078	Overtone of Amide II
2940-2915	2938	2935	2939	2936	2939	2933	2937	2934	2939	Symmetric C-H stretching of CH_3
2885-2865	2879	2885	2883	2877	2877	2880	2882	2881	2883	Asymmetric C-H stretching of CH_2
1703-1697	1700	1700	1700	1699	1699	1699	-	-	-	Antiparallel β-sheet
1700-1600	1618	1618	1619	1618	1618	1619	1639	1640	1639	Amide I C=O stretching
1580-1510	1515	1515	1515	1515	1516	1515	1517	1525	1527	Amide II N-H bending (wagging) plus C-N stretching
1480-1440	-	-	-	-	-	-	1453	1457	1456	C-H deformation (scissoring)
1440-1260	1402	1401	1399	1398	1400	1395	1393	1393	1394	C-H and O-H bending vibration
1305-1200	1238	1240	1241	1239	1243	1238	1242	1247	1247	Amide III N-H bending (twisting) plus C-N stretching and contribution from O=C-N bending
1090-1000	1068	1069	1069	1068	1068	1067	1072	1072	1074	C-OH stretching vibration

Notes: me = methanol, et = ethanol, and *iso-* = *iso*-propanol

4.7.3 Secondary structure of silk sericin microparticles analyzed by ATR FT-IR microspectroscopy

The Amide I region in the range between 1740-1580 cm^{-1} was chosen as a representative for secondary structure analysis. The number and location of individual bands obtained from second derivative of original spectra were used in curve fitting. The curve fitting of silk sericin microparticles spectra in the Amide I region obtained from boiling solution of silk fiber with distilled water after treated with different organic solvents are shown in Figure 4.9. Each Amide I component assignments are based on the prior study. According to curve fitting, the Amide I bands are classified to aggregate β-strand, β-sheet (intramolecular), random coil, α-helix, β-turn, and antiparallel β-sheets. The peaks at ~1648, ~1662, and ~1617 cm^{-1} are assigned to random coil and α-helix, and aggregate β-strand, respectively. In general, alcohol can induce the structural changes of proteins upon hydrogen bond induction [44]. Accordingly, precipitation of sericin solution in organic solvents can induce structural changes from random coil to aggregate β-strand with strong intermolecular hydrogen bonds among extended chains. Strong hydrogen bonds involving C=O stretching is represented by negative shift of Amide I bands when sericin solution was treated with organic solvents, in terms of lower electron density in the C=O group [26]. The band at highest frequency (1700 cm^{-1}) is assigned to the antiparallel β-sheet and the absorption band at 1683 cm^{-1} is assigned to β-turn. Similarly, degumming with citric acid the curves fitting of the obtain microparticles are shown in Figure 4.10. Although the curves fitting are the same, the proportions of secondary structure depend on degumming agents. Degumming with distilled water, the aggregated β-strand contents of silk sericin microparticles treated with *iso*-propanol, ethanol, and methanol are 37.71%, 40.46%, and 41.23%, respectively. The proportion of random coil component is highest when silk sericin microparticles were treated with *iso*-propanol. Degumming with citric acid, the aggregated β-strand contents of silk sericin microparticles treated with *iso*-propanol, ethanol, and methanol were increased sequentially as 37.80 %, 38.85 %, and 41.38 %, respectively. The proportion of random coil component was highest when silk sericin microparticles were treated with *iso*-propanol. The proportions of secondary structures are summarized in Table 4.5 and 4.6. It can be concluded that the order of effective solvents for forming

aggregated β-strand is methanol > ethanol > *iso*-propanol regardless of degumming agents.

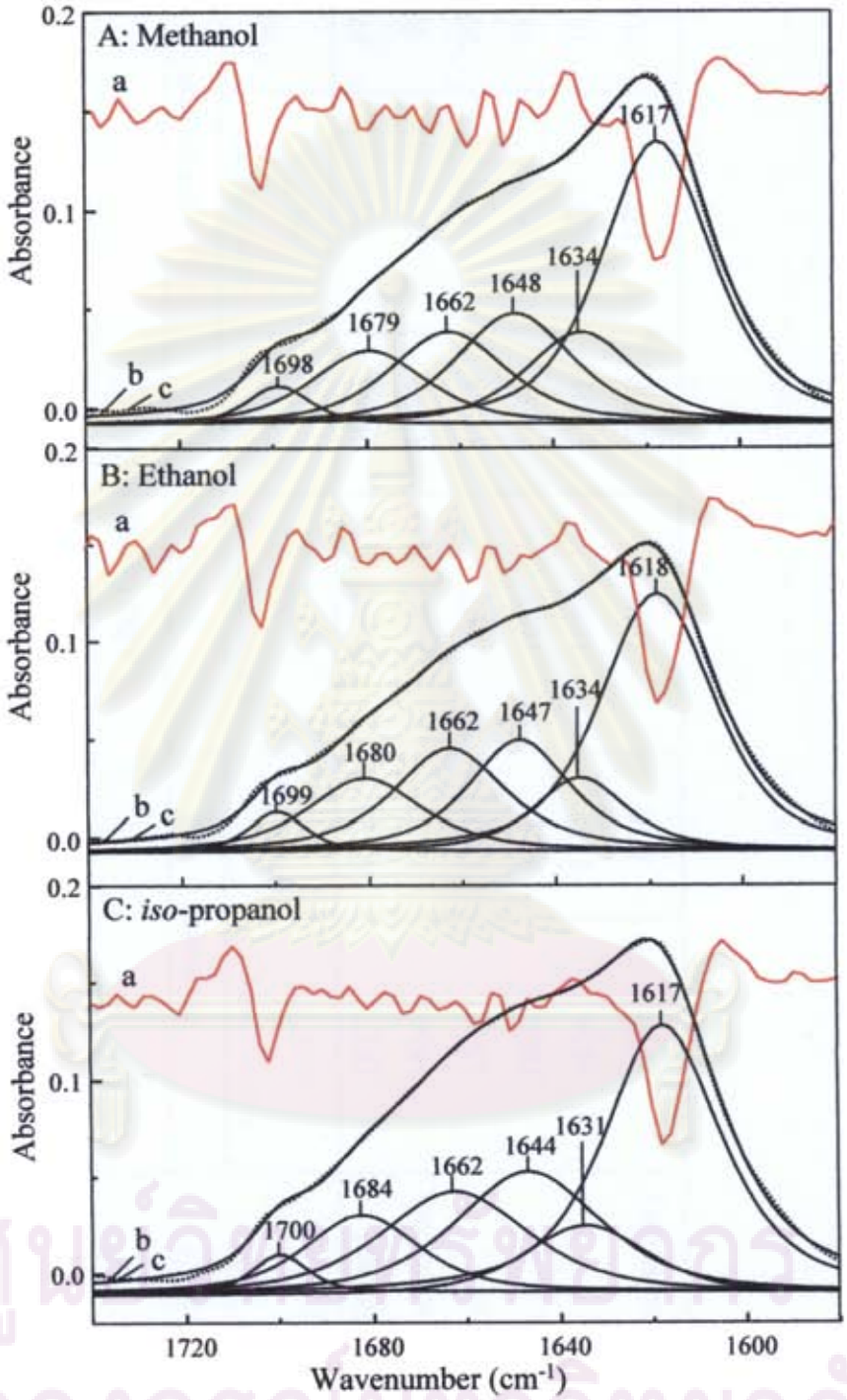

Figure 4.9 Curve fitting of silk sericin microparticles spectra in the Amide I region obtained from boiling solution of silk fiber with distilled water after treated with (A) methanol, (B) ethanol, and (C) *iso*-propanol: (a) second derivative spectrum, (b) deconvolved (solid line) spectrum, and (c) original (dotted line) spectrum.

Table 4.5 Carbonyl absorption associated with the secondary structure of silk sericin microparticles obtained from boiling solution of silk fiber with distilled water after treated with different organic solvents [16, 19, 41].

Literatures	Assignments	silk sericin microparticles obtained from boiling solution of silk fiber with distilled water after treated with					
		methanol		ethanol		*iso*-propanol	
		wavenumber (cm^{-1})	Area (%)	wavenumber (cm^{-1})	Area (%)	wavenumber (cm^{-1})	Area (%)
1605-1627	Aggregate β-strand	1617	41.23	1618	40.46	1617	37.71
1628-1637	β-sheets (Intramolecular)	1634	13.33	1634	11.90	1631	9.84
1638-1655	Random coil	1648	17.01	1647	17.84	1644	20.64
1656-1662	α-helix	1662	14.19	1662	14.96	1662	18.25
1663-1696	β-turn	1679	11.09	1680	11.95	1684	10.59
1697-1703	β-sheets (Intermolecular)	1698	3.16	1699	2.89	1700	2.97

ศูนย์วิทยทรัพยากร
จุฬาลงกรณ์มหาวิทยาลัย

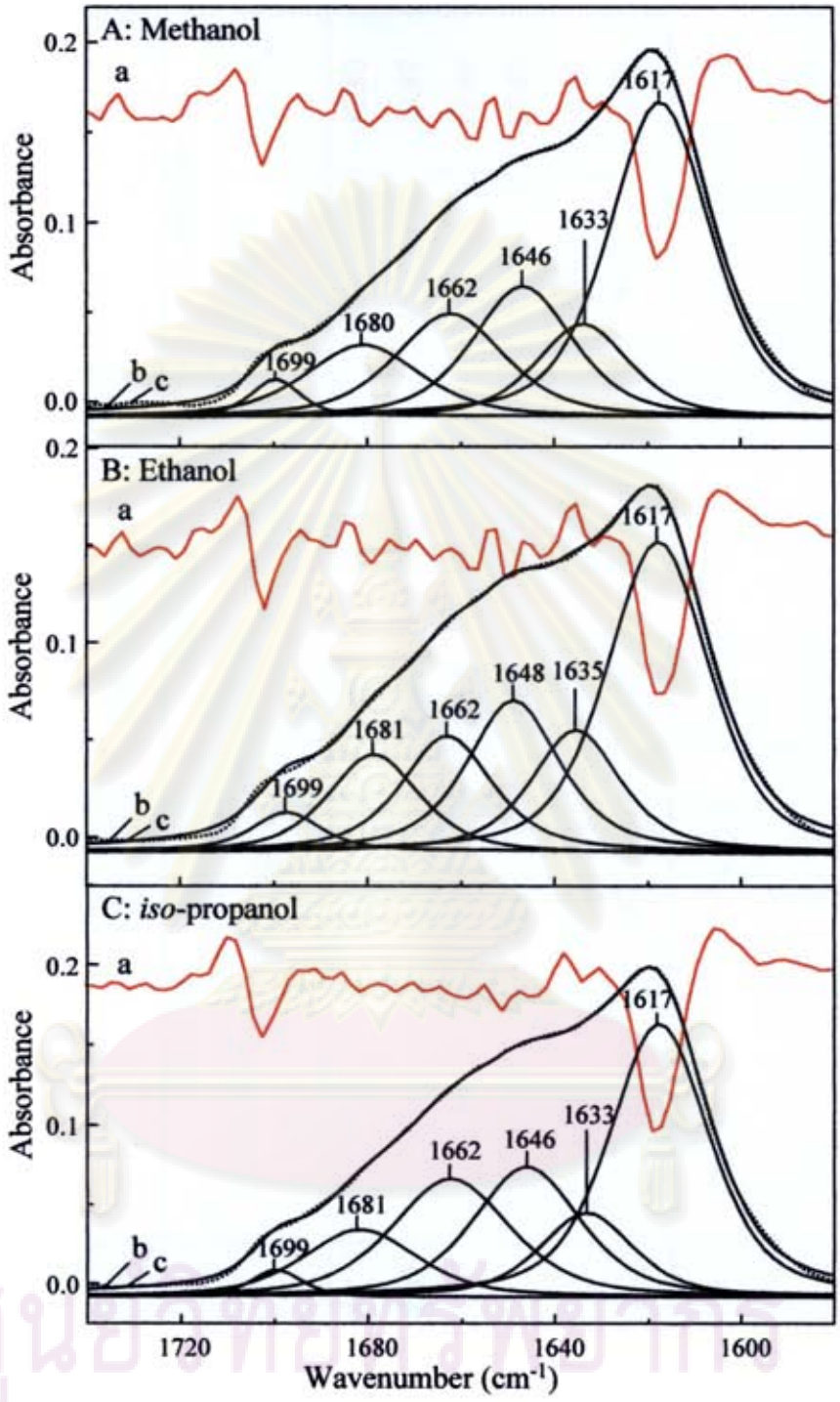

Figure 4.10 Curve fitting of silk sericin microparticles spectra in the Amide I region obtained from boiling solution of silk fiber with citric acid after treated with (A) methanol, (B) ethanol, and (C) *iso*-propanol: (a) second derivative spectrum, (b) deconvolved (solid line) spectrum, and (c) original (dotted line) spectrum.

Table 4.6 Carbonyl absorption associated with the secondary structure of silk sericin microparticles obtained from boiling solution of silk fiber with citric acid after treated with different organic solvents [16, 19, 41].

Literatures	Assignments	silk sericin microparticles obtained from boiling solution of silk fiber with citric acid after treated with					
		methanol		ethanol		*iso*-propanol	
		wavenumber (cm^{-1})	Area (%)	wavenumber (cm^{-1})	Area (%)	wavenumber (cm^{-1})	Area (%)
1605-1627	Aggregate β-strand	1617	41.38	1617	38.85	1617	37.80
1628-1637	β-sheets (Intramolecular)	1633	11.51	1635	13.35	1633	10.97
1638-1655	Random coil	1646	17.42	1648	18.51	1646	19.44
1656-1662	α-helix	1662	15.82	1662	15.97	1662	19.40
1663-1696	β-turn	1680	11.05	1681	10.96	1681	10.50
1697-1703	β-sheets (Intermolecular)	1699	2.82	1699	2.53	1699	1.88

ศูนย์วิทยทรัพยากร
จุฬาลงกรณ์มหาวิทยาลัย

The curve fitting of silk sericin microparticles spectra in the Amide I region obtained from boiling solution of silk fiber with $NaHCO_3$ after treated with methanol, ethanol, and *iso*-propanol are shown in Figure 4.11. The curve fitting of silk sericin microparticles spectra in Amide I regions are summarized in Table 4.7. Secondary structure of silk sericin microparticles are classified to the aggregate β-strand, intramolecular β-sheet, random coil, α-helix, and β-turn. The peaks at 1646 and 1659 cm^{-1} have been assigned to random coil and α-helix, respectively. The peaks at 1625 and 1635 cm^{-1} are attributed to aggregated β-strand and β-sheet (intramolecular), respectively. Moreover, the absorption bands at 1670 cm^{-1} and 1685 cm^{-1} are assigned to be β-turn. The intramolecular β-sheets have a random coil in which the hydrogen bond is weaker than intermolecular hydrogen bonds. It is very easy to absorb water molecules that induce the structural changes of protein i.e. the folded structure becomes unfolded structure and then transforms into β-structure. The aggregate β-strand contents of silk sericin microparticles after treated with *iso*-propanol, ethanol, and methanol were increased sequentially as 10.86%, 13.92%, and 19.72%, respectively. The proportion of random coil component was highest when sericin microparticles were treated with *iso*-propanol. The α-helix structures are composed of 17.99%, 15.97%, and 26.82% in silk sericin microparticles treated with methanol, ethanol, and *iso*-propanol, respectively.

In summery, the sericin microparticles were prepared by precipitating of sericin solution obtained from boiling silk fiber with distilled water and citric acid, thus transformed into aggregated β-strand when treated with organic solvents. The structure is fixed by intermolecular hydrogen bonding and still remains of crystallization when the water molecules are removed. The sericin microparticles obtained from sericin solution degumming with $NaHCO_3$ does not form intermolecular hydrogen bonds. It is expected that $NaHCO_3$ hydrolyzes polypeptides into small molecules, and the sericin microparticles after treated with organic solvents do not form interchain hydrogen bonds with other polar side chains.

ศูนย์วิทยทรัพยากร
จุฬาลงกรณ์มหาวิทยาลัย

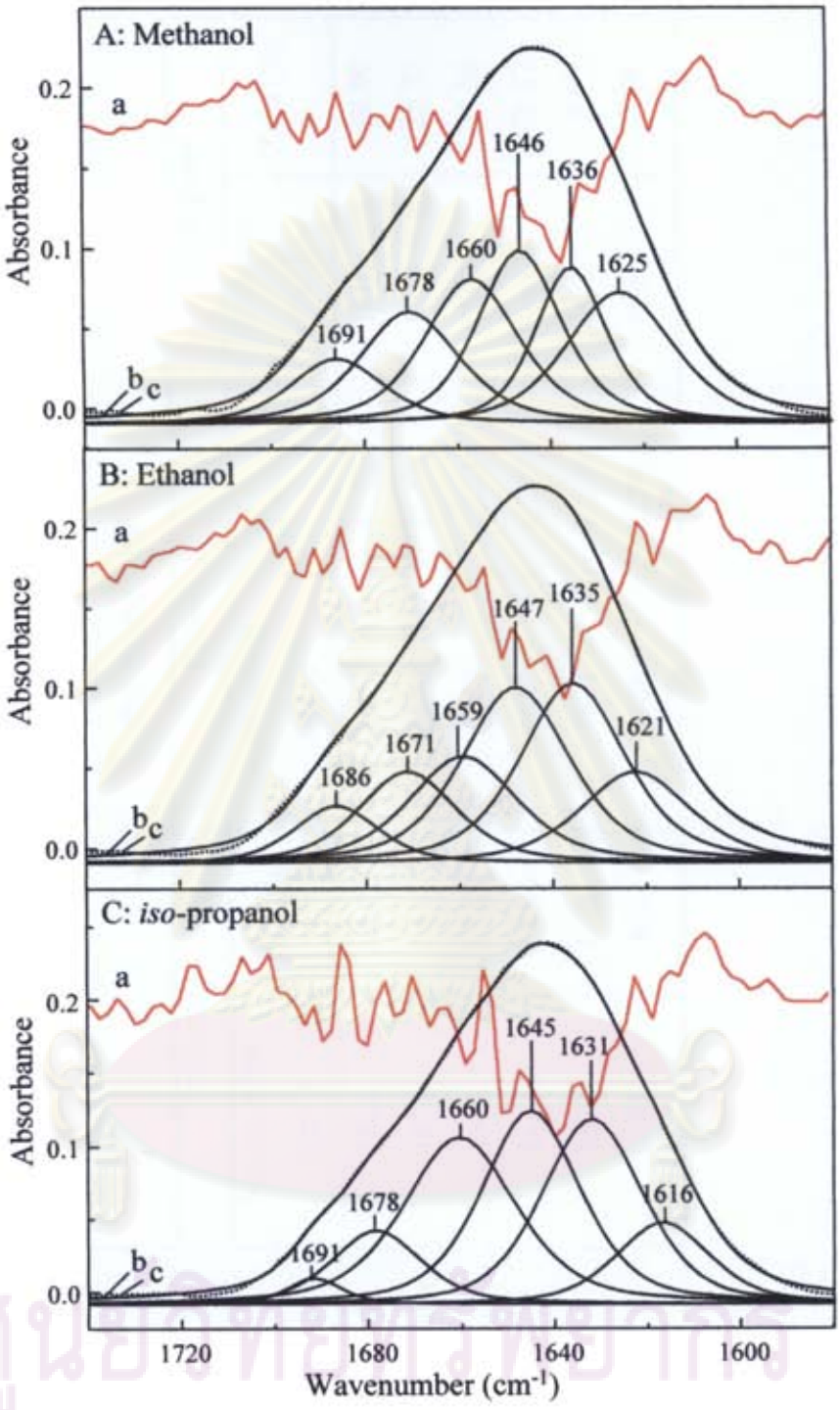

Figure 4.11 Curve fitting of silk sericin microparticles spectra in the Amide I region obtained from boiling solution of silk fiber with $NaHCO_3$ after treated with (A) methanol, (B) ethanol, and (C) *iso*-propanol: (a) second derivative spectrum, (b) deconvolved (solid line) spectrum, and (c) original (dotted line) spectrum.

Table 4.7 Carbonyl absorption associated with the secondary structure of silk sericin microparticles obtained from boiling solution of silk fiber with $NaHCO_3$ after treated with different organic solvents [16, 19, 41].

Literatures	Assignments	silk sericin microparticles obtained from boiling solution of silk fiber with citric acid after treated with					
		methanol		ethanol		*iso*-propanol	
		wavenumber (cm^{-1})	Area (%)	wavenumber (cm^{-1})	Area (%)	wavenumber (cm^{-1})	Area (%)
1605-1627	Aggregate β-strand	1625	19.72	1621	13.92	1616	10.86
1628-1637	β-sheets (Intramolecular)	1636	18.49	1635	25.69	1631	25.77
1638-1655	Random coil	1646	19.99	1647	25.61	1645	24.98
1656-1662	α-helix	1660	17.99	1659	15.97	1660	26.82
1663-1696	β-turn	1678	15.51	1671	12.28	1678	9.49
1697-1703	β-turn	1691	8.30	1686	6.54	1691	2.08

ศูนย์วิทยทรัพยากร
จุฬาลงกรณ์มหาวิทยาลัย

After the microparticles were prepared, the mass of product has been measured. The yield of silk sericin microparticles was determined according to Equation 4.1

$$\%\text{yield} = \left(\frac{\text{weight of product}}{\text{weight of silk sericin}} \right) \times 100 \qquad (4.1)$$

For example;

No. # 1

Weight of silk sericin = 0.742 g

Weight of silk sericin microparticles = 0.408 g

$$\% \text{ yield} = \frac{0.408 \times 100}{0.742}$$

$$= 54.98$$

No. # 2

Weight of silk sericin = 0.534 g

Weight of silk sericin microparticles = 0.339 g

$$\% \text{ yield} = \frac{0.339 \times 100}{0.534}$$

$$= 63.48$$

Average yield = 59.23%

The yield of silk sericin microparticles with different preparative conditions are shown in Table 4.8. Degumming with citric acid gives the best mass product (~50-60% yield).

Table 4.8 The average yield of silk sericin microparticles treated with organic solvents.

Degumming agent	The average yield of silk sericin microparticles		
	Methanol	Ethanol	*iso*-propanol
Distilled water	30.34	28.79	28.20
Citric acid	59.23	55.14	50.95
$NaHCO_3$	25.40	22.26	20.88

4.8 ATR FT-IR spectra of native silk sericin and silk sericin microparticles obtained from treatment with methanol

ATR FT-IR spectrum of native silk sericin in comparison with the spectrum of silk sericin microparticles after treated with methanol are shown in Figure 4.12. Degumming with distilled water and citric acid, the Amide I band of the obtained silk sericin microparticles is narrower than that of the native silk sericin. It can be concluded that sillk sericin microparticles have more β-sheet structure than that of the native silk sericin because organic solvents can induce the forming of intermolecular hydrogen bonds. Since sericin does not form an oriented structure by the natural spinning of silkworm, treatment with organic solvents can induce the formation of aggregated strands that transfer the stretching stress through their strong intermolecular hydrogen bonds generating an oriented structure. On the other hand, the obtained silk sericin microparticle degumming with $NaHCO_3$ does not show structural changes to β-sheet structure. Silk fiber boiled with $NaHCO_3$ can degrade sericin polypeptides into small amino acid. Therefore, sericin solution does not pack to molecular chain in sericin segment after precipitation in organic solvents.

ศูนย์วิทยทรัพยากร
จุฬาลงกรณ์มหาวิทยาลัย

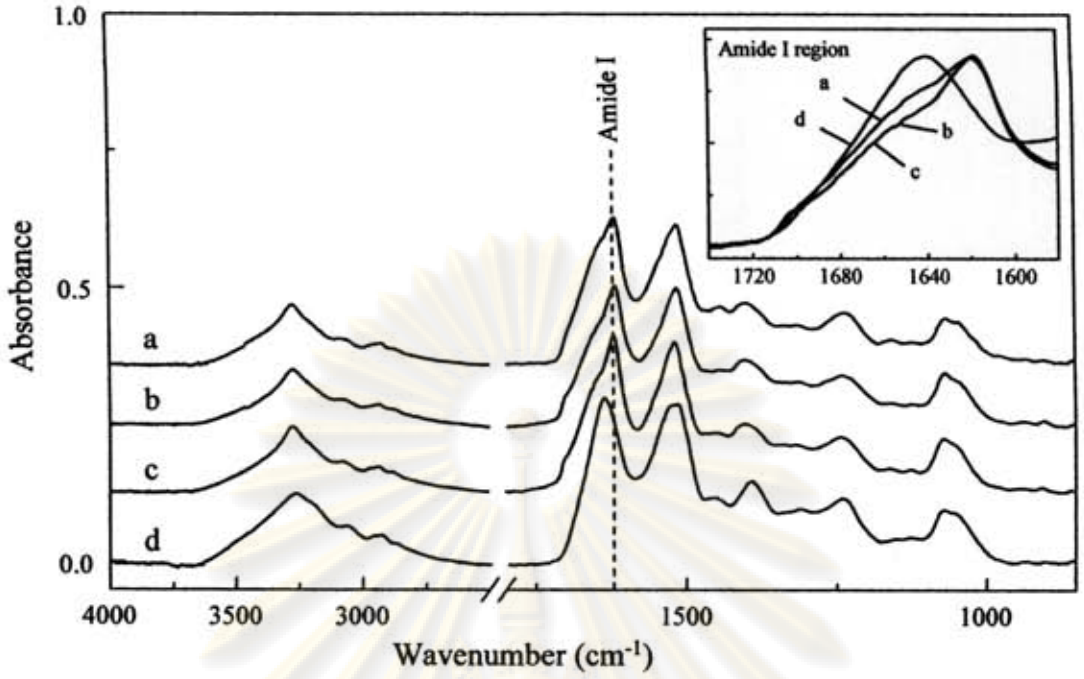

Figure 4.12 ATR FT-IR spectra of (a) native silk sericin; silk sericin microparticles obtained by precipitating of sericin solution in methanol with different degumming agent: (b) distilled water, (c) citric acid, and (d) $NaHCO_3$. The inset is the normalized spectra in Amide I region.

4.9 The deposition of silver nanoparticles on silk sericin microparticles

Silver nanopartilcles are produced by Sensor Research Unit, Chulalongkorn University. They were deposited on sericin microparticles. The deposition of silver nanoparticles was analyzed by transmission electron microscope and UV-Visible spectroscopy. Concentrations of silver nanoparticles utilized in experiment were 50, 100, and 200 ppm. Figure 4.13 shows the images of deposited silver nanoparticles on silk sericin microparticles.

ศูนย์วิทยทรัพยากร
จุฬาลงกรณ์มหาวิทยาลัย

Figure 4.13 The deposited silver nanoparticles on silk sericin microparticles with concentrations: (a) 50, (b) 100, and (c) 200 ppm.

4.9.1 TEM images of silver nanoparticles deposited on silk sericin microparticles

TEM images of silk sericin microparticles based on magnification images (×5, ×20, and ×100) are shown in Figure 4.14 (A). The organic solvents were removed from silk sericin microparticles by centrifugation. Silk sericin microparticles can be damaging during centrifugation because they can absorb water and get swollen again such that the particles of silk sericin cannot observe on TEM image. TEM images of silver nanoparticles deposited on sericin microparticles with different concentration (50, 100, and 200 ppm) are shown in Figure 4.14 (B, C, D). The silver nanoparticles were spherical shape with an average diameter of the particles of 10 nm. The images show that silver nanoparticles are well dispersed and deposit very well on silk sericin microparticles. With the concentration of 200 ppm of silver nanoparicles, they can be deposited greater on silk sericin microparticles than that of 100 ppm and 50 ppm. It makes sense that the deposited product is proportional to the original amount of nanoparticles.

ศูนย์วิทยทรัพยากร
จุฬาลงกรณ์มหาวิทยาลัย

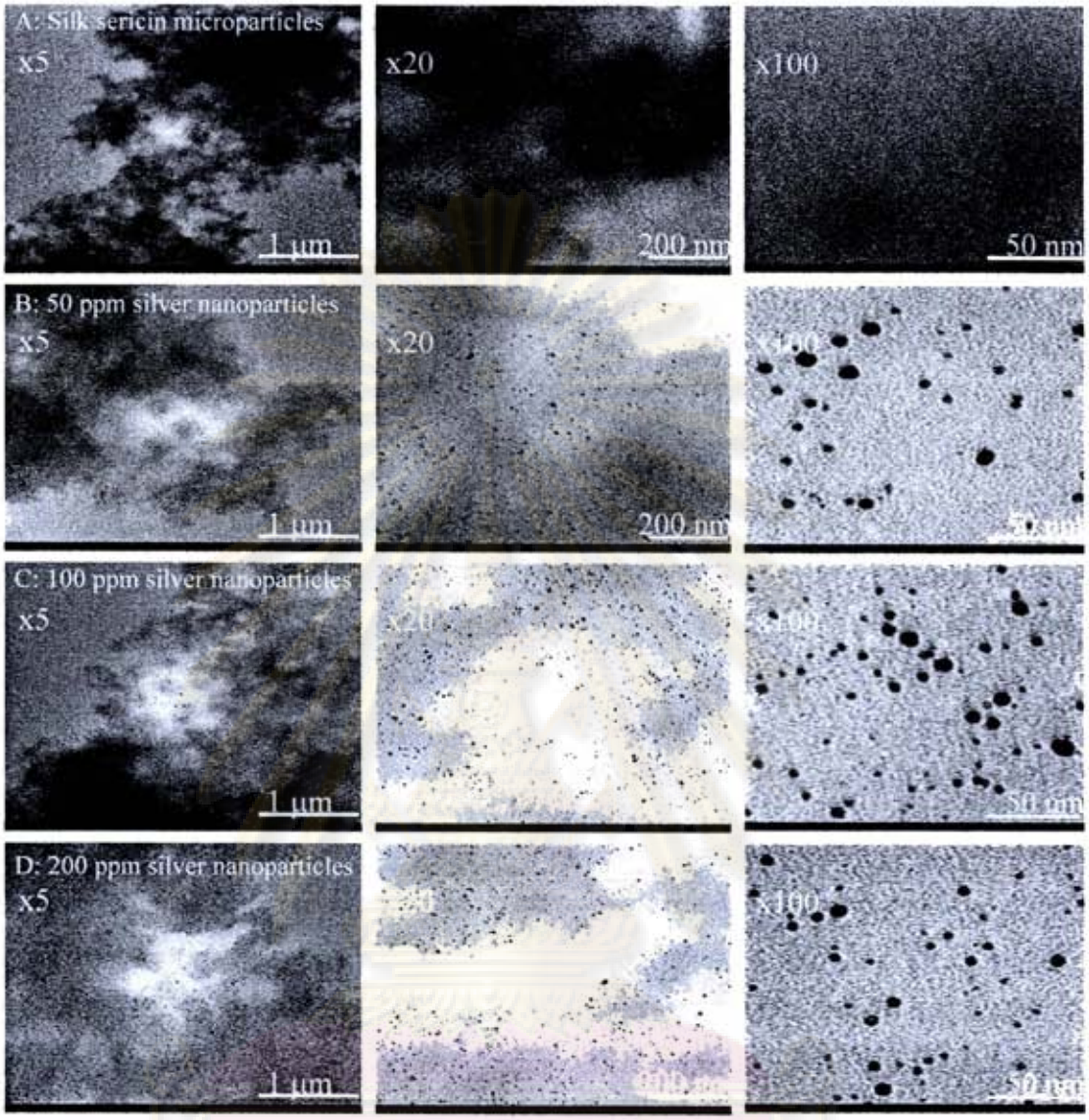

Figure 4.14 Transmission electron microscope (TEM) images of (A) silk sericin microparticles and the silver nanoparticles deposited on silk sericin microparticles with concentrations (B) 50, (C) 100, and (D) 200 ppm.

ศูนย์วิทยทรัพยากร
จุฬาลงกรณ์มหาวิทยาลัย

4.9.2 The ATR FT-IR spectra of silk sericin microparticles before and after added silver nanoparticles

The ATR FT-IR spectra of silk sericin microparticles before and after added silver nanoparticles are shown in Figure 4.15. After the deposition of silver nanoparticles, the small shoulder peaks at 1154 and 1045 cm^{-1} appear which are more intense with increasing in the concentration of nanoparticles. These two peaks are

assigned to C-O and C-O-C stretching vibration of starch as a stabilizer of silver nanoparicles. The Amide I band is getting broader when the concentrations of deposited nanoparticles increase. The broad band at 1617 cm^{-1} of silk spectra after adding with silver nanoparticles indicates capping manner of the nanoparticles [47]. These because silver nanoparticles can be inserted into the sericin structures and induce the loosely packing of polypeptide chains.

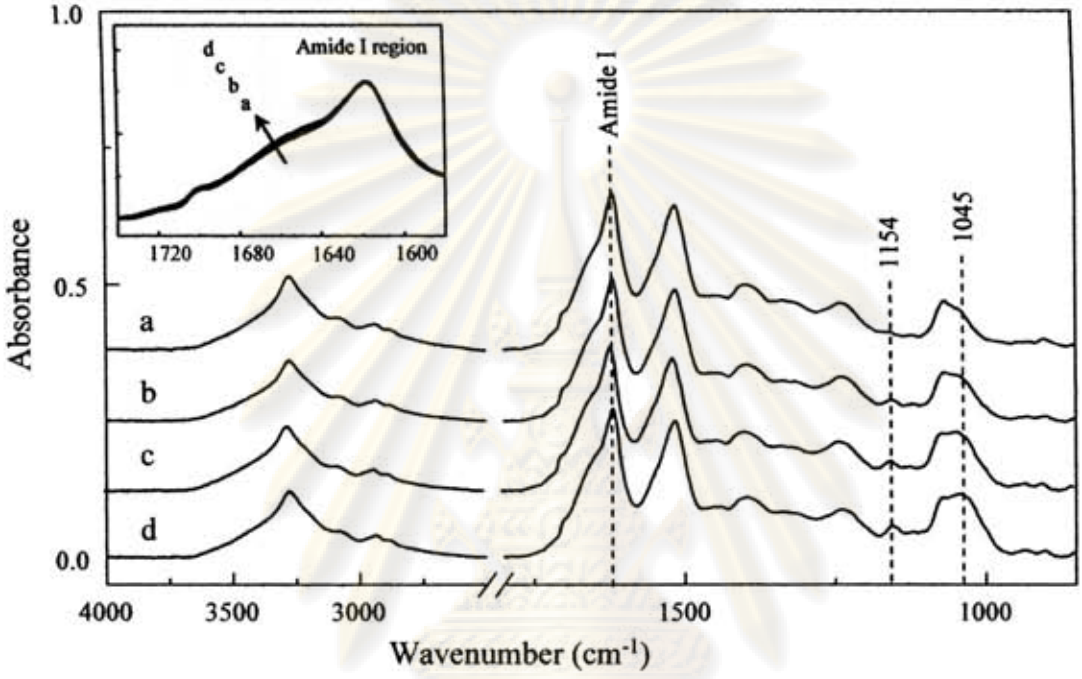

Figure 4.15 ATR FT-IR spectra of (a) silk sericin microparticles and silver nanoparticles deposited on silk sericin microparticles with concentrations: (b) 50, (c) 100, and (d) 200 ppm.

4.9.3 UV-Vis spectra of silver nanoparticles before and after deposited on silk sericin microparticles and the release of silver nanoparticles deposited on silk sericin microparticles

Silver nanoparticles solutions have maxima absorption (λ_{max}) at 400 nm. Figure 4.16 shows the UV-Vis spectra of silver nanoparticles, silver nanoparticles residue in distilled water, and the release of silver nanoparticles deposited on silk sericin microparticles after added with distilled water. The absorbance spectra of silver nanoparticles were used to calculate the amount of silver nanoparticles deposited on

silk sericin microparticles. The deposition of silver nanoparticles on silk sericin microparticles is increased when increasing the concentration of silver nanoparticles.

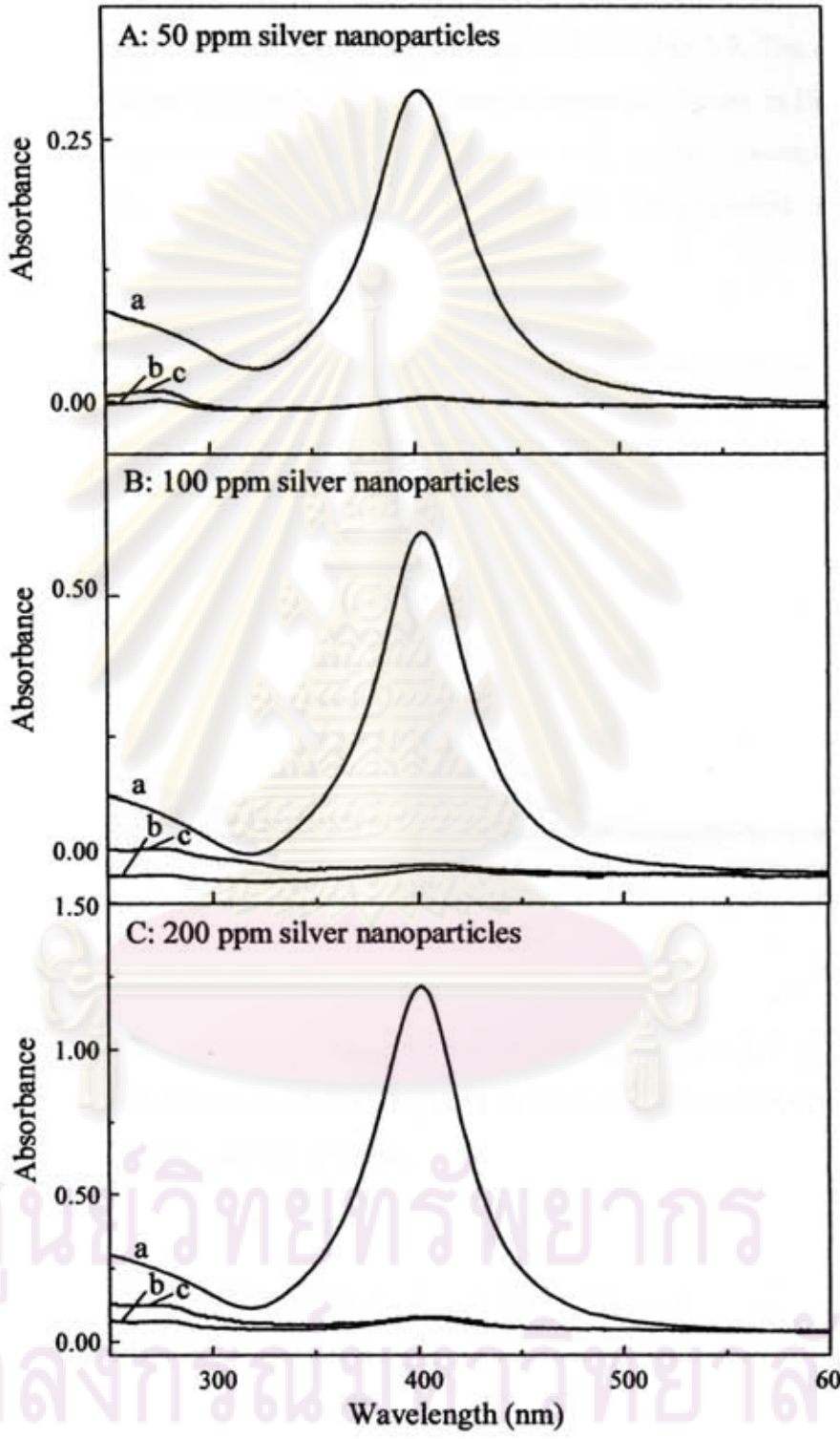

Figure 4.16 UV-Vis absorption spectra of (A) 50, (B) 100, and (C) 200 ppm silver nanoparticles: (a) reference, (b) silver nanoparticles residue in distilled water, and (c) the release of silver nanoparticles deposited on silk sericin microparticles.

ศูนย์วิทยทรัพยากร
จุฬาลงกรณ์มหาวิทยาลัย

4.10 UV-Vis spectra of silver nanoparticles at different concentrations

Figure 4.17 shows the UV-Vis spectra of silver nanoparticles at different concentrations. Absorbencies of spectra are summarized in Table 4.9. The calibration curves of silver nanoparticles with different concentrations are shown in Figure 4.18. The volume of deposited silver nanoparticles on silk sericin microparticles is calculated from the calibration curve according to "straight-lined equations" (y = mx+c).

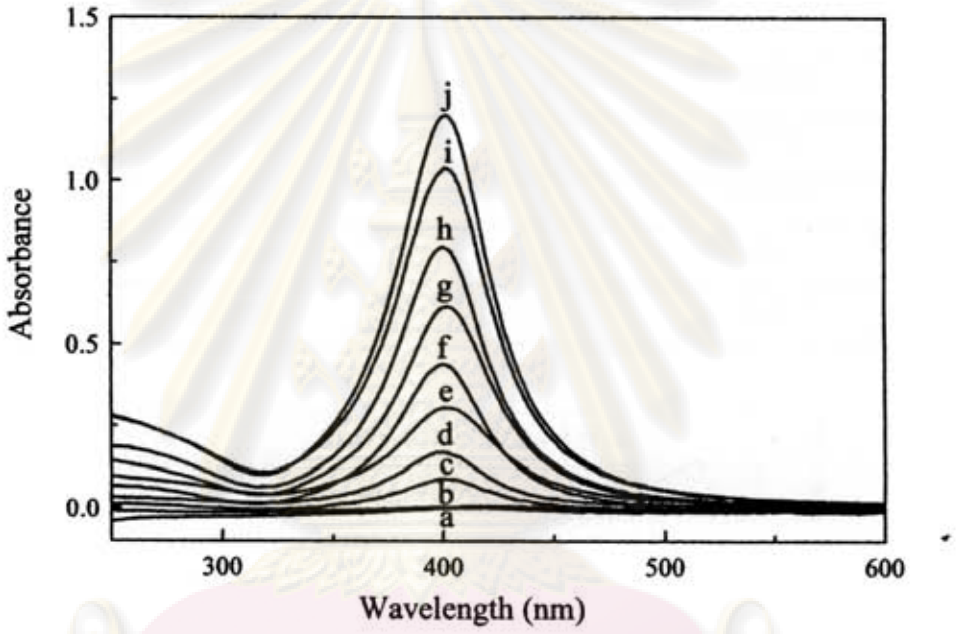

Figure 4.17 UV-Vis absorption spectra of silver nanoparticles at different concentrations of: (a) 0.05, (b) 0.25, (c) 0.5, (d) 1.5, (e) 2.5, (f) 3.5, (g) 5, (h) 6.5, (i) 8, and (j) 10 ppm.

ศูนย์วิทยทรัพยากร
จุฬาลงกรณ์มหาวิทยาลัย

Table 4.9 The absorbance of UV-Vis spectra of silver nanoparticles at different concentrations.

Silver concentration (ppm) 20 times dilution with distilled water	Absorbance
0.05 ppm	0.006
0.25 ppm	0.020
0.5 ppm	0.078
1.5 ppm	0.169
2.5 ppm	0.307
3.5 ppm	0.438
5 ppm	0.616
6.5 ppm	0.796
8 ppm	1.012
10 ppm	1.213

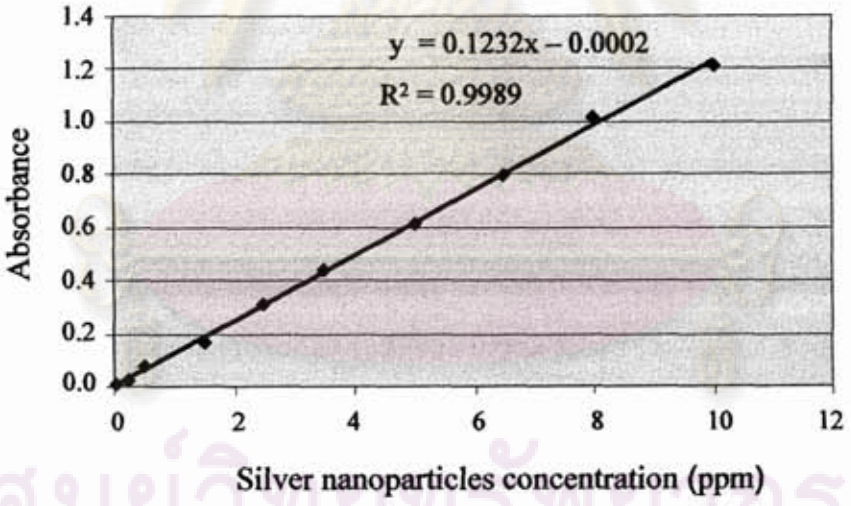

Figure 4.18 Calibration curve of silver nanoparticles at different concentrations.

The Equation 4.2 was fitted to a linear equation of the intensity dependent of silver nanoparticles, which was used to calculate the concentrations of silver nanoparticles added into silk sericin microparticles.

$$y = 0.1232x - 0.0002 \quad (4.2)$$

4.11 The deposition of silver nanoparticles on silk sericin microparticles and the release of silver nanoparticles deposited on silk sericin microparticles

In order to determine the amount of the deposited silver nanoparticles on silk sericin microparticles, 10 mL of silver nanoparticles was added into 2 mL of silk sericin microparticles suspended with distilled water. The average weights of silk sericin microparticles suspension were 0.063±0.01 g. Table 4.10 shows the weight of silver nanoparticles deposited on sericin microparticles. From these result, the weight of silver nanoparticles deposited on silk sericin microparticles increased with increasing in concentration of silver nanoparticles. The depositions were confirmed by adding 10 mL of distilled water into silver nanoparticles deposited on silk sericin microparticles. After that silver nanoparticles deposited on silk sericin microparticles were release. Table 4.11 shows the release of silver nanoparticles deposited on silk sericin microparticles.

Weight of silver can be calculated as follows:

$$\text{Weight of silver}(\mu g) = \text{silver concentration}(ppm) \times \text{volume of silver solution}(mL) \quad (4.3)$$

50 ppm silver nanoparticles were 20 times dilution
with distilled water = 2.5 ppm
Weight of silver = 25 μg (1)
Weight of silver residue in distilled water = 0.58 μg (2)
Deposition of silver nanoparticles (μg)/silk 0.063 g = 24.42 μg (1)-(2)
Deposition of silver nanoparticles (μg)/silk 1 g = 387.62 μg (3)

The weights of the release of silver nanoparticles on silk sericin microparticles are calculated from weight of silver equation. Absorbance of silver nanoparticles released into distilled water is equal to 0.008

Silver nanoparticles releases into distilled water = 0.067 ppm (1)
Release of silver nanoparticles (μg)/silk 0.063 g = 0.67 μg (2)
Release of silver nanoparticles (μg)/silk 1 g = 10.63 μg (3)

ศูนย์วิทยทรัพยากร
จุฬาลงกรณ์มหาวิทยาลัย

Table 4.10 Deposition of silver nanoparticles on silk sericin microparticles.

Silver concentration after 20 times dilution	Absorbance of silver nanoparticles		Weight ((μg) of silver nanoparticles		Deposition of silver nanoparticles (μg)/silk 0.063 g	Deposition of silver nanoparticles (μg)/silk 1 g
	Before deposition	After deposition	Before deposition	After deposition		
2.5 ppm	0.307	0.007	25	0.58	24.42	387.62
5 ppm	0.616	0.011	50	0.91	49.09	779.21
10 ppm	0.1213	0.026	100	2.13	97.87	1553.49

Table 4.11 The release of silver nanoparticles after deposition on silk sericin microparticles.

Silver concentration (ppm) after 20 times dilution	Absorbance of silver nanoparticles added with distilled water	Silver weight (μg) added with distilled water	The release of silver nanoparticles (μg)/silk 0.063 g	The release of silver nanoparticles (μg)/silk 1 g
2.5 ppm	0.007	0.58	0.58	9.21
5 ppm	0.016	1.31	1.31	20.79
10 ppm	0.023	1.88	1.88	29.84

The summary of deposition and release of silver nanoparticles on sericin microparticles are shown in Table 4.12.

Table 4.12 The summary of deposition and release of silver nanoparticles on silk sericin microparticles.

Silver concentration (ppm)	Deposition of silver nanoparticles (μg)/silk 1 g	The release of silver nanoparticles (μg)/silk 1 g
50 ppm	7,752.4	184.2
100 ppm	15,457.2	415.8
200 ppm	31,069	596.8

ศูนย์วิทยทรัพยากร
จุฬาลงกรณ์มหาวิทยาลัย

CHAPTER V

CONCLUSIONS

The relationship between molecular conformation and the secondary structure of native silk sericin fiber and silk sericin microparticles are elucidated by means of ATR FT-IR microspectroscopy. The native silk sericin has more the random coil and α-helix structure than that of silk fibroin fiber. These results indicated that the native silk sericin had less crystalline structure compared to that of silk fibroin fiber. Silk sericin microparticles were obtained from precipitation of sericin solution in organic solvents. The sericin solution was prepared from boiling of silk fiber with degumming agent. Using $NaHCO_3$ as degumming agent, the soluion did not separate sericin into two proportions. With distilled water and citric acid, sericin solutions were seperated into two proportions (α-sericin and β-sericin). In this work, the preparation of silk sericin microparticles by precipitating in organic solvent was developed. The color of silk sericin microparticles obtained from degumming silk fiber with $NaHCO_3$ is yellow while it is white when degumming with distilled water and citric acid. The different color was also correlated with the results of ATR FT-IR spectra of microparticles in which the spectrum of microparticles precipitating from sericin solution degumming with $NaHCO_3$ was different from that of microparticles spectra obtained after degumming with distilled water and citric acid. The observed ATR FT-IR spectra of the silk sericin microparticles obtained from degumming silk fiber with distilled water and citric acid after treating with methanol, ethanol, and *iso*-propanol indicated the increment of β-sheet conformation. This may associated with the packing of molecular chain. It was found that the secondary structure of microparticles precipitated in methanol were the riches of aggregate β-strand, while precipitating in *iso*-propanol were the riches of random coil structure. The microparticles obtained from degumming silk fiber with $NaHCO_3$ did not show β-sheet conformation because $NaHCO_3$ could degrade polypeptides into small amino acid which could not induce the packing of molecular chain. The particle sizes of silk sericin microparticles are in the range of microparticle scale. The particles size of silk sericin distributed from 3-8 μm and the average size is about 5 μm.

Application of silver nanoparticles deposited on silk sericin microparticles. The results of Amide I band of silk sericin microparticles added with silver nanoparticles have broad band indicating the capping manner of silver nanoparticles by silk sericin microparticles.

ศูนย์วิทยทรัพยากร
จุฬาลงกรณ์มหาวิทยาลัย

REFERENCES

[1] Vaithanomsat, P.; and Kitpreechavanich, V. Sericin separation from silk degumming wastewater. *Sep. Purif. Technol.* 59 (2008):129-133.

[2] Wu, J.H.; Wang, Z.; and Xu, S.Y. Preparation and characterization of sericin powder extracted from silk industry wastewater. *Food Chem.* 103 (2007):1255-1262.

[3] Fabiani, C.; Pizzichini, M.; Spadoni, M.; and Zeddita, G. Treatment of waste water from silk degumming processes for protein recovery and water reuse. *Desalination* 105 (1996): 1-9.

[4] Zhang, Y.Q. Applications of natural silk sericin protein in biomaterial. *Biotechnol. Adv.* 20 (2002): 91-100.

[5] Zhang, Y.Q.; Mu, Y.; Xia, Y.Y.; Shen, W.D.; Mao, J.P.; and Xue, R.Y. Silk sericin-insulin bioconjugates: Synthesis, characterization and biological activity. *J. Control. Release* 115 (2006): 307-315.

[6] Kongdee, A.; Bechtold, T.; and Teufel, L. Modification of cellulose fiber with silk sericin. *J. Appl. Polym. Sci.* 96 (2005): 1421-1428.

[7] Gulrajani, M. L.; Brahma, K. P.; Kumar, P.S.; and Purwar, R. Application of Silk Sericin to Polyester Fabric *J. Appl. Polym. Sci.* 109 (2008): 314-321.

[8] Komatsu, K. Studies on dissolution behaviors and structural characteristic of silk sericin. *Bull. Sericult. Exp. Sta.* 26 (1975): 135-256.

[9] Teramoto, H.; Nakajima, K.I.; and Takabayashi, C. Preparation of elastic hydrogel. *Biosci. Biotechnol. Biochem.* 69 (4) (2005): 845-847.

[10] Kongdee, A.; Okubayashi, S.; Tabata, I.; and Hori, T. Impregnation of silk sericin into polyester fibers using supercritical carbon dioxide. *J. Appl. Polym. Sci.* 105 (2007): 2091-2097.

[11] Sarovart, S.; Sudatis, B.; Meesilpa, P.; Grady, B.P.; and Magaraphan R. The use of sericin as an antioxidant and antimicrobial for polluted air treatment. *Rev.Adv.Mater.Sci.* 5 (2003): 193-198.

[12] Anghileri, A.; Lantto, R.; Kruus, K.; Arosio, K.; and Freddi, G. Tyrosinase-catalyzed grafting of sericin peptides onto chitosan and production of protein–polysaccharide bioconjugates. *J. Biotechnol.* 127 (2007): 508-519.

[13] Sonthisombat, A.; and Speakman, P. Silk: Queen of fibres - the concise story. p.1-28. Cited in Sandoz colour chronicle. October/December 1990, p.1-4 and 16-19.

[14] Lamoolphak, W.; De-Eknamkul, W.; and Shotipruk, A. Hydrothermal production and characterization of protein and amino acids from silk waste. *Bioresour. Technol.* 99 (2008): 7678-7685.

[15] Sheng, J.; Lin, H.; Wang, L.; Yu, Y.; and Hu, H. Study on the microstructure and physical chemical properties of diffluent sericin powder. *Textile Industry Publishing House* 6 (2000): 6-9.

[16] Teramoto, H.; and Miyazawa, M. Analysis of structural properties and formation of sericin fiber by infrared spectroscopy. *J. Insect Biotechnol. Sericol.* 72 (2003):157-162.

[17] Cho, K.Y.; Moon, J.Y.; Lee, Y.W.; Lee, K.G.; Yeo, J.H.; Kweon, H.Y.; Kim, K.H.; and Cho, C.S. Preparation of self-assembled silk sericin nanoparticles. *Int. J. Biol. Macromol.* 32 (2003): 36-42.

[18] Lee, K.G.; Kweon H.Y.; Yeo J.H.; Woo S.O.; Lee Y.W.; Cho C.S.; Kim K.H.; and Park Y.H. Effect of methyl alcohol on the morphology and conformational characteristics of silk sericin. *Int. J. Biol. Macromol.* 33 (2003): 75-80.

[19] Teramoto, H.; and Miyazawa, M. Molecular orientation behavior of silk sericin film as revealed by ATR infrared spectroscopy. *Biomacromolecules* 6 (2005): 2049-2057.

[20] Kurioka, A.; Kurioka, F.; and Yamazaki, M. Characterization of sericin powder prepared from citric acid-degraded sericin polypeptides of the silkworm, *Bombyx Mori. Biosci. Biotechnol. Biochem.* 68 (2004): 774-780.

[21] The silkworm shop [online]. Available from: www.silkwormshop.com/ silkworm_info.html.

[22] Mondal, M.; rivedy, K.; and Kumar, S.N. The silk proteins, sericin and fibroin in silkworm, *Bombyx mori* Linn., A Review *Caspian J. Env. Sci.* 5 (2007): 63-76.

[23] Robson, R.M. Handbook of Fibre Science and Technology. New York: Mercel Dekker Inc, 1985.

[24] Gulrajani, M.L. Department of Textile Technology Indian Institute of Technology, New Delhi. *Degumming of silk; in Silk dyeing printing and finishing, M.L. Gulrajani (ed)* (1988):63-95.

[25] Freddi, G.; Mossotti, R.; and Innocenti, R. Degumming of silk fabric with several proteases. *J. Biotechnol.* 106 (2003): 101-112.

[26] Zhang, Y.Q.; Tao, M.L.; Shen, W.D.; Zhou, Y.Z.; Ding, Y.; Ma, Y.; and Zhou W.L. Immobilization of L-aspararaginase on the microparticles of the natural silk sericin protein and its characters. *Biomaterials.* 25 (2004): 3751-3759.

[27] Mishra, S.P. Mishra. A Text Book of Fibre Science and Technology. New Delhi: New Age Publishers, 2000.

[28] Milani, K. Peptide bonds-card 28 [online]. Available from: www.hcc.mnscu.edu /chem/V.27/page_id_27148.html.

[29] Raghava, G.P.S.; and Kaur, H. A server for β-turn types predition. [online]. Available from: www.imtech.res.in/raghava/betaturns/turn.html.

[30] Whitford, D. Proteins Structure and Function. Chichester: John Wiley & Sons, 2005.

[31] Seidman, L. Chapter 2: Protein structure. [online]. Available from: http://matcmadison.edu/biotech/resources/proteins/labManual/chapter_2. html.

[32] Urban, M. W. Attenuated Total Reflectance Spectroscopy of Polymer: Theory and Practice. Washington: American Chemical Society, 1996.

[33] Harrick, N. J. (Ed.). Internal Reflection Spectroscopy. New York: Harrick Scientific Corporation, 1979.

[34] Huang, J.; Valluzzi, R.; Bini, E.; Vernaglia, B.; and Kaplan, D.L. Cloning, Expression, and Assembly of sericin-like protein. *J. Biol. Chem.* 278 (2003): 46117-46123

[35] Monti, P.; Freddi, G.; Arosio, C.; Tsukada, M.; Arai, T.; and Taddei, P. Vibrational spectroscopic study of sulphated silk proteins. *Journal of Molecular Structure* 834-836 (2007): 202-206.

[36] Socrates, G. Infrared and Raman Characteristic Group Frequencies Table and Charts. Chichester: John Wiley & Sons, 2001.

[37] Grath, K.M.; Kaplan, D. Protein-Based Material. Boston: Birkhauser, 1997.

[38] Byler, D.M.; and Susi, H. Examination of the secondary structure of proteins by deconvolved FTIR spectra. *Biopolymers* 25 (1986): 469-487.

[39] Surewicz, W.K.; and Mantsch, H.H. New insight into protein secondary structure from resolution-enhanced infrared spectra. *Biochim. Biophys. Acta* 952 (1988): 115-130.

[40] Surewicz, W.K.; Mantsch, H.H. and Chapman, D. Determination of protein secondary structure by Fourier transform infrared spectroscopy: critical assessment. *Biochemistry*. 32 (1993):389-394.

[41] Hu, X.; Kaplan, D.; and Cebe, P. Determining beta-sheet crystallinity in fibrous proteins by thermal analysis and infrared spectroscopy. *Macromolecules* 39 (2006): 6161-6170.

[42] Bose, P.C.; Majumdar, S.K.; and Sengupta, K. Role of the amino acids in silkworm, *bombyx mori* L. nutrition and their occurrence in haemolymph, silk gland and silk cocoons –A Review. *Indian J. Seric.* 28 (1989): 17-31.

[43] Sadov, F; Korchagin, M.; and Matetsky, A. Chemical technology of fibrous materials. Moscow: Mir Publication, 1987.

[44] Teramoto, H.; Kakazu, A.; Yamanchi, K.; and Asakura, T. Role of hydroxyl side chains in *bombyx mori* silk sericin in stabilizing its solid structure. *Macromolecules* 39 (2006): 6161-6170.

ศูนย์วิทยทรัพยากร
จุฬาลงกรณ์มหาวิทยาลัย

[45] Grigshy, J.J.; Blanch, H.W.; and Prausnitz, J.M. Cloud-point temperatures for lysozyme in electrolyte solutions: effect of salts type, salt concentration and pH. *Biophys. Chem.* 32 (2001): 231-43.

[46] Kim, U.J.; Park, J.; Kim, H.J.; Wada, M.; and Kaphan, D.L. Three-dimensional aqueous-derived biomaterial scaffolds from silk fibroin. *Biomaterials.* 26 (2005): 2775-2785.

[47] Dong, Q.; Su, H.; and Zhang, D. In situ depositing silver nanoclusters on silk fibroin fibers supports by a novel biotemplate redox technique at room temperature. *J. Phys. Chem.* 109 (2005): 17429-17434.

ศูนย์วิทยทรัพยากร
จุฬาลงกรณ์มหาวิทยาลัย

APPENDICES

ศูนย์วิทยทรัพยากร
จุฬาลงกรณ์มหาวิทยาลัย

APPENDICES

1. Amino structure

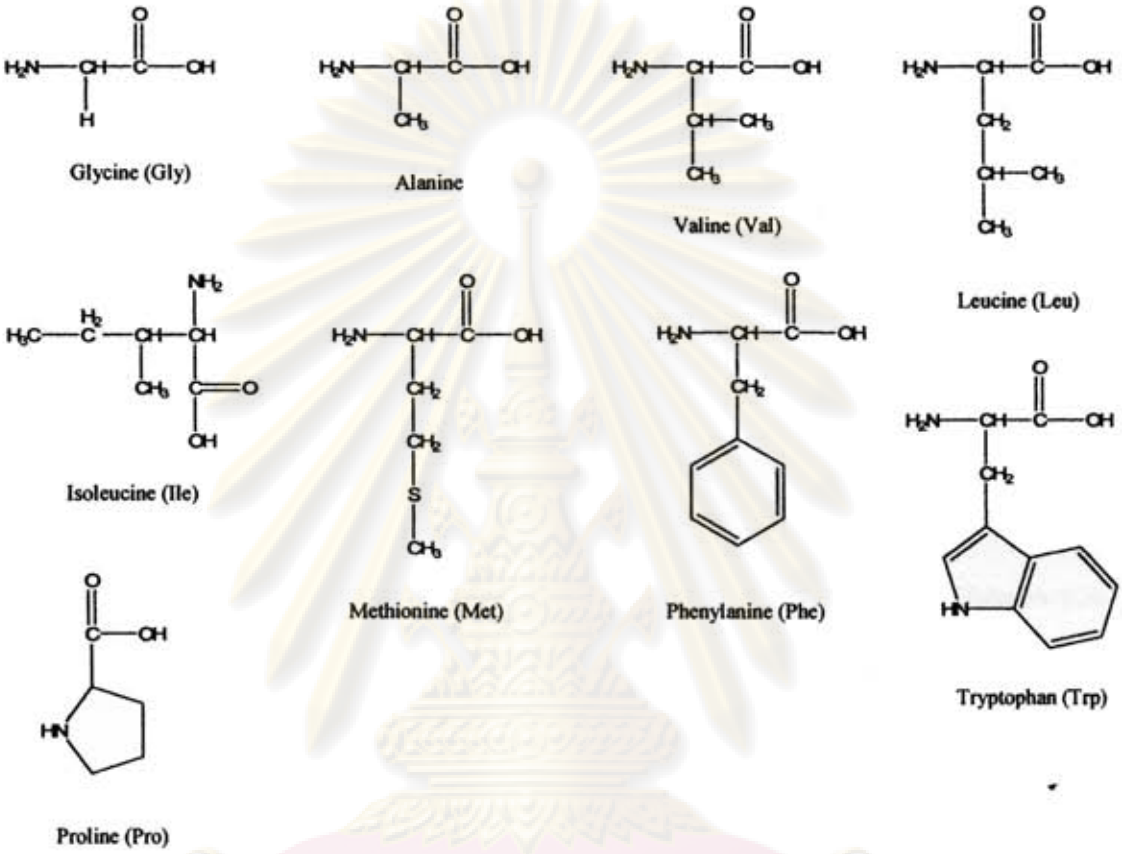

Figure A1. Non-polar amino acid.

ศูนย์วิทยทรัพยากร
จุฬาลงกรณ์มหาวิทยาลัย

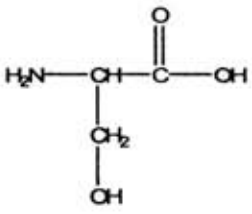

Serine (Ser)

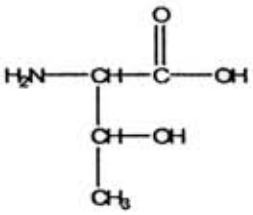

Threonine (Thr)

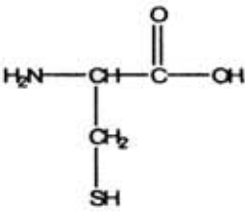

Cysteine (Cys)

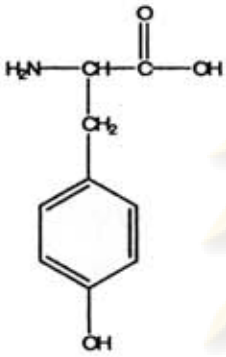

Tyrosine (Tyr)

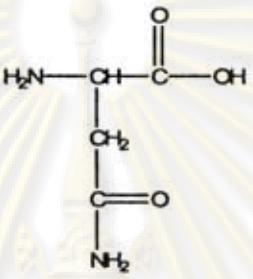

Asparagine (Asn)

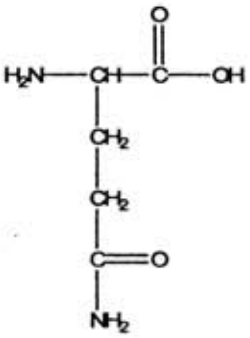

Glutamine (Gln)

Figure A2. Polar amino acid.

ศูนย์วิทยทรัพยากร
จุฬาลงกรณ์มหาวิทยาลัย

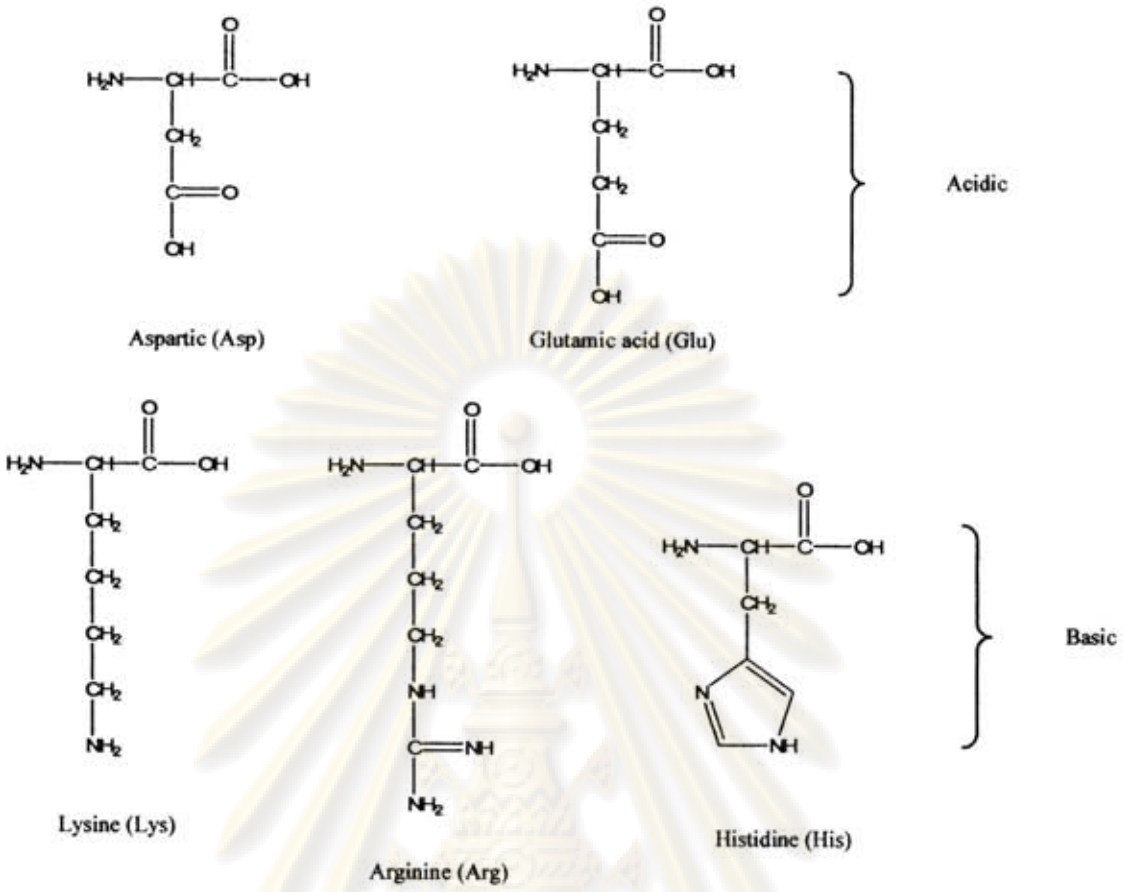

Figure A3. Electrically charged amino acid.

2. Henderson-Hasselbalch Equation, we can calculate the net charge on serine at pH 3.0, 7.0 and 10.0

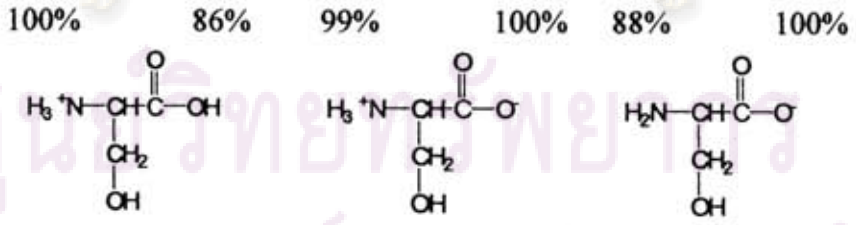

pH 3.0 Net charge +1

pH 7.0 Net charge 0

pH 10.0 Net charge -1

ศูนย์วิทยทรัพยากร
จุฬาลงกรณ์มหาวิทยาลัย

3. Polarity of solvent

ศูนย์วิทยทรัพยากร
จุฬาลงกรณ์มหาวิทยาลัย

CURRICULUM VITAE

Name: Miss Seeliya Limtoprasert

Date of Birth: May, 28th, 1983, Singburi, Thailand
Father: Mr. Mongkorn Limtoprasert
Mather: Mrs. Ranu Limtoprasert

Address: 79/42 Royalpark2 Condominium Rangnam Road, Soi Sodpinson Phayathai, Rattevee Bangkok 10400
E-mail address: seeliya_sl@hotmail.com

Education:

2006	Bachelor of Engineering (Petrochemicals and Polymeric Materials), Silpakorn University, Nakornpathom, Thailand
2008	Master of Science (Petrochemistry and Polymer Science), Chulalongkorn University, Bangkok, Thailand

Conference:

May 2007	Polymer Graduate Conference of Thailand, Faculty of Science, Mahidol University, Salaya, Thailand.
October 2007	The 33rd Congress on Science and Technology of Thailand (STT.33) Walailak University, Nakorn Si Thammarat, Thailand.
September 2007	National Research Council of Thailand, Thailand Research Expo, Central World Plaza, Bangkok, Thailand.
December 2007	International Graduate Congress 2007, 3rd MPSGC, Faculty of Science, University of Malaya, Kuala Lumpur.
March 2008	The 15th Academic Conference, the 2007 Annual Meeting, Faculty of Science, Chulalongkorn University, Thailand.